

MTP-AERO-62-49  
June 5, 1962

216

N64-24047

code 1

Cat. 12

TMX51724

Cat. 12

*50p*  
**GEORGE C. MARSHALL**

**SPACE  
FLIGHT  
CENTER**

**HUNTSVILLE, ALABAMA**

**WIND FLOW IN THE 80-400 KM ALTITUDE REGION  
OF THE ATMOSPHERE**

By

George C. Ragsdale

and

Peter E. Wasko

LIBRARY COPY

AUG 17 1962

LANGLEY RESEARCH CENTER  
LI  
NASA  
LAMP STATION  
HAMP. VIRGINIA

**OTS PRICE**

XEROX

\$

4.60 ph

MICROFILM

\$

**NASA**

**NATIONAL AERONAUTICS AND SPACE ADMINISTRATION**

GEORGE C. MARSHALL SPACE FLIGHT CENTER

MTP-AERO-62-49

WIND FLOW IN THE 80-400 KM ALTITUDE REGION  
OF THE ATMOSPHERE

By

George C. Ragsdale  
and  
Peter E. Wasko

ABSTRACT

24047

An attempt is made in this report to deduce the wind characteristics in the 80-400 km ionospheric region of the atmosphere for the purpose of establishing wind input data for launch vehicle and spacecraft design and performance studies. Although the amount of wind data available is far from that desirable for such an undertaking, there is a sufficient amount of data to give at least an indication of the probable wind characteristics at these high atmospheric levels. In this report the most important wind measurement techniques are described, the wind data obtained from recent rocket techniques and from a literature survey of ionospheric drift measurements are presented, the probable maximum wind speed envelope is established, the wind shears are determined, and some general wind flow characteristics are deduced.

*Author*

GEORGE C. MARSHALL SPACE FLIGHT CENTER

---

MTP - AERO - 62 - 49

---

WIND FLOW IN THE 80-400 KM ALTITUDE REGION  
OF THE ATMOSPHERE

by

George C. Ragsdale  
and  
Peter E. Wasko

SPACE ENVIRONMENT SECTION  
AEROPHYSICS AND ASTROPHYSICS BRANCH  
AEROBALLISTICS DIVISION

## TABLE OF CONTENTS

	Page
SECTION I. INTRODUCTION	2
SECTION II. TECHNIQUES OF MEASUREMENT	3
A. Acoustic Method	4
Rocket Grenade	4
B. Visual Methods	5
1. Sodium Vapor Trails	5
2. Meteor Trails	6
3. Noctilucent Clouds	6
C. Radio Methods	7
1. Chaff	7
2. Meteor Trails	7
3. Radio-Fading	8
4. Sporadic-E	8
5. Radio-Star Scintillation Method	9
SECTION III. PRESENTATION AND DISCUSSION OF DATA	9
A. Wind Flow Characteristics	9
1. Speed and Direction Variations	9
2. Wind Vector Variations	10
3. Zonal and Meridional Wind Component Variations	12
4. Additional Summer and Winter Ionospheric Winds in the 80-400 km Region	14
5. Extreme Winds	16
6. Wind Shear and Turbulence	16
SECTION IV. CONCLUSIONS	18

## LIST OF ILLUSTRATIONS

Figure	TITLE	Page
1.	Rocket-Grenade Technique of Measuring Winds . . . .	21
2.	Sodium Vapor Technique of Measuring Winds . . . . .	22
3.	Chaff Technique of Measuring Winds . . . . .	23
4.	Meteor Trail Technique of Measuring Winds . . . . .	24
5.	Radio-Fading Technique of Measuring Winds . . . . .	25
6.	Wind Speed Curves Obtained from Sodium Vapor Trail Measurements at Wallops Island, Virginia . . . .	26
7.	Wind Direction Curves Obtained from Sodium Vapor Trail Measurements at Wallops Island, Virginia . . . . .	27
8.	Wind Speed Envelopes Obtained from Sodium Vapor Trail Measurements at Wallops Island, Virginia . . . .	28
9.	Aerogram of Wind Vectors Obtained from Sodium Vapor Trail (Wallops Island, Va.; Holloman AFB, N. M.; Eglin AFB, Fla.) and Chaff (Tonopah, Nev.) Measurements . . . . .	29
10.	Aerogram of Wind Vectors Obtained from Sodium Vapor Trail (Wallops Island, Va.; Holloman AFB, N. M.; Eglin AFB, Fla.) and Chaff (Tonopah, Nev.) Measurements . . . . .	30
11.	Mean Zonal Wind Cross Section for the 30°-40° North Latitude Belt . . . . .	31
12.	Mean Meridional Wind Cross Section for the 30°- 40° North Latitude Belt . . . . .	32
13.	Aerogram of Wind Vector Based on Ionospheric Drift and Meteor Trail Drift Observations . . . . .	33

ERRATA

MTP-AERO-62-49

"WIND FLOW IN THE 80-400 KM ALTITUDE REGION  
OF THE ATMOSPHERE"

By

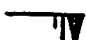
George C. Ragsdale

Peter E. Wasko

June 5, 1962

ures 9, 10 and 13: Insert at top of each figure the following:

LEGEND

 - Wind speed from east, 65 m/sec

ures 11 and 12: Insert at end of caption in each figure the following:

(Wind Speed in m/sec)

EXTERNAL

Mr. Willis Webb  
USASMSA  
Missile Meteorology Division  
White Sands Proving Ground, N. M.

GEORGE C. MARSHALL SPACE FLIGHT CENTER

MTP-AERO-62-49

WIND FLOW IN THE 80-400 KM ALTITUDE REGION  
OF THE ATMOSPHERE

By

George C. Ragsdale  
And  
Peter E. Wasko

SUMMARY

As much wind data as possible were obtained in the 80-400 km ionospheric region of the atmosphere, and by various techniques, summarized into useful forms for interpretation and deducing wind flow characteristics in these high atmospheric regions for use in space vehicle design studies. As a first approximation, the deductions of the wind flow characteristics in this region, based on this study, can be applied to the Cape Canaveral, Florida, area.

The most important wind measurement techniques presently used are described in the first part of the report. Wind data obtained by the sodium vapor trail method are presented and discussed with respect to wind direction, wind speed, wind vector, and wind shear characteristics. Monthly mean zonal and meridional cross-sections for the 30-40 degree latitude belt were constructed for the 80-200 km region and interpreted. Additional winds above 200 km from ionospheric drift measurements and from some recent sodium vapor trail measurements are used to deduce wind flow conditions in the 200-400 km region.

The most important deductions of the wind flow characteristics in the 80-400 km region are summarized and presented in the section on conclusions.



## SECTION I. INTRODUCTION

Winds and wind shears represent one of the most important inputs to launch vehicle and spacecraft design and performance studies. For this reason, it is desirable to have an understanding of the wind flow and to obtain wind speed and wind shear profiles from the surface to the maximum altitude of available data. From the wind data, values for the standardized parameters used in the various design studies (Ref. 1) can be obtained.

The 80-400 km atmospheric region investigated in this report lies in the ionosphere. The ionosphere is divided into regions designated as D, E, and F. The ionosphere between 60 and 85 km is the D-region, that between 85 and 140 km the E-region, and that above 140 km the F-region, which in turn, is divided into the F<sub>1</sub> and F<sub>2</sub> regions. The F<sub>1</sub> region lies between 140 and 200 km, and the F<sub>2</sub> region lies between 200 and 1300 km (Ref. 2). In addition, a sporadic E layer (E<sub>s</sub>), a few kilometers in thickness, occurs rather frequently near 100 km as a local intensification of the electron concentration (as much as twice) above that in the ambient E-layer.

Measurements made from rockets and satellites (Ref. 3) show that these layers or ledges of electrons with electron concentration peaks are not as distinct as formerly thought. Instead, there appears to exist a rather densely ionized region without any very well-defined layers. However, since much of the ionospheric wind data (Ref. 4-28) is identified and located in altitude according to the former ionospheric model, the established letter designation will be used in this report mainly to identify a particular altitude region.

Data for the region of the atmosphere above 80 km are sparse and relatively little is known about winds and wind shears at these high altitudes. Therefore, an attempt is made in this report to estimate the probable wind flow characteristics in the 80-400 km ionospheric region based upon information made available from a variety of measurement techniques.

# List of Illustrations (Continued)

Figure	TITLE	Page
14.	Probable Maximum Wind Speed Envelope from 60 to 400 km .....	34
15.	Wind Shear Envelopes Obtained from Sodium Vapor Trail Measurements at Wallops Island, Virginia, for 500 m Altitude Layers ( $\Delta h$ ) .....	35
16.	Wind Shear Envelopes Obtained from Sodium Vapor Trail Measurements at Wallops Island, Virginia, for 1000 m Altitude Layers ( $\Delta h$ ) .....	36
17.	Wind Shear Envelopes Obtained from Sodium Vapor Trail Measurements at Wallops Island, Virginia, for 3000 m Altitude Layers ( $\Delta h$ ) .....	37
18.	Wind Shear Envelopes Obtained from Sodium Vapor Trail Measurements at Wallops Island, Virginia, for 5000 m Altitude Layers ( $\Delta h$ ) .....	38

The authors wish to gratefully acknowledge that the sodium vapor trail wind data for Wallops Island, Virginia, were made available by Dr. W. Nordberg and Mr. W. S. Smith, Aeronomy and Meteorology Division, Goddard Space Flight Center, and Dr. E. R. Manring, Physics Research Division, Geophysics Corporation of America; and those for Eglin AFB, Florida, by Dr. K. S. W. Champion, Office of Aerospace Research, AF Cambridge Research Laboratory. Also, gratitude is expressed to Mr. Thomas A. King for his invaluable assistance in computing and checking some of the data and in plotting many of the graphs used in this report.

## SECTION II. TECHNIQUES OF MEASUREMENT

Various methods are employed to obtain wind measurements in the atmosphere. A number of techniques were summarized and illustrated in Reference 29. Most wind speed and wind shear profiles for the lower atmosphere (surface to 30 km) are determined from conventional rawinsonde measurement. These sounding balloons have yielded a considerable amount of data from the surface up to 30 km, with a few measurements up to 40 km. More recent techniques utilizing angle-of-attack, spherical balloon-radar and smoke and vapor trail observations have been used to supplement the balloon data in this altitude range. Winds in the altitude region between 30 and 80 km have been measured primarily by the use of (1) large explosions on the ground, (2) sounding rockets ejecting grenades, parachutes, balloons, or chaff, and (3) to a lesser extent, by smoke and sodium vapor trail photography.

Some data from 30 to 60 km are from the anomalous propagation-of-sound measurement from large explosions on the ground. Rocket-grenade, parachute, balloon, and chaff experiments have been the primary source of data gathering between about 40 and 80 km of altitude. Noctilucent clouds are found at high latitudes, and give wind measurements between 74 and 92 km. From about 80 to 110 km, there are data from meteor trails and ionospheric drifts. Sporadic-E measurements are

usually made at an altitude near 100 km. Sodium vapor ejected from rockets allows wind measurements to be made between 30 and about 250 km, depending on the maximum height capability of the rocket. Although not statistically adequate, these data provide a first estimate for space vehicle design studies of winds and wind shears to be expected at these altitudes. From 200 km up to about 400 km, the data are primarily from ionospheric drifts.

The rocket-grenade and chaff techniques are included in the following description of some techniques of measurements since they are also used to sample the atmosphere a little above 80 km.

#### A. ACOUSTIC METHOD

**Rocket-Grenade:** In the region of the atmosphere between 30 and 90 km, the rocket-grenade method has been a primary source of wind measurements. This method employs a rocket that carries a number of grenades in its nose cone. The grenades are ejected from the rocket's nose cone at various altitudes and explode almost immediately. When the grenades explode, a spherical wave-front is generated (see Fig. 1). Due to the wind movement in the atmosphere, the wave-front is distorted as it propagates toward the ground. When the wave-front arrives at the surface of the earth, ground-based microphones record the sound. By properly tracing the explosion back to its point of origin, a wind profile of the traversed media can be constructed.

The average winds in a medium between two high-altitude grenade explosions are determined by measuring exactly the time of explosion of each grenade, the time and direction of arrival of each sound wave at a number of ground-based microphones, and the exact position of each grenade explosion. The position and time data of each grenade explosion can be gotten from a single station DOVAP (Doppler velocity and position) transmitter-receiver and a single ballistic camera (Ref. 30). From the recorded data on the Doppler shift of the 73.8 Mc radiation transmitted from the moving rocket to the ground, the slant range to the rocket (the grenade detonation position relative to the rocket is known) can be

determined very accurately; and, from the use of the camera, the direction cosines of the grenade explosion can be obtained. The azimuth position and altitude (see Fig. 1) of the grenade are then established. The time of explosion is observed on the DOVAP cycle-count record as an electro-magnetic radiation interference pattern resulting from the explosion; and, the time of arrival of the sound wave is recorded by each of five microphones arranged in a shape of a symmetric cross. Generally, three microphones are sufficient to determine the angle of arrival of the wave front. A more sophisticated all weather observing system is described in Reference 31.

## B. VISUAL METHODS

1. Sodium Vapor Trails. Direct wind measurements in the upper atmosphere above 110 km are very scarce. In the past few years measurements have been obtained up to an altitude of 230 km at Wallops Island, Virginia, by ejecting a continuous sodium vapor trail into the earth's upper atmosphere from a rocket (Ref. 32, 33, 34). Measurements have also been obtained at Eglin AFB, Florida (Ref. 35) and Holloman AFB, New Mexico (Ref. 36).

The trail extends over a large altitude range allowing the determination of a relatively complete wind profile. The lower limit is determined by aerodynamic effects since the initial injection of the sodium vapor may cause instability during the early part of the flight. The upper limit of the trail is determined by the capability of the vehicle. The positions of the trail at various altitudes and times are obtained from an analysis of photographs taken simultaneously from at least two widely separated locations, and three or more are desirable (Ref. 32). This technique is illustrated in Figure 2.

The exact locations of distinct points on the ejected cloud are usually determined by placing three projectors on a scale model site and focusing the corresponding negatives simultaneously on a screen (Ref. 32). The height of the point on the vapor trail is determined by a special table designed to take into account the ground coordinates. To make certain that the projectors are

correctly orientated, a star field is photographed just before launching the rocket. From the projected image positions of the stars, the projectors can be aligned relative to one another as were the cameras in the field.

2. Meteor Trails. Wind measurements from meteor trails can be obtained by photographic techniques. Whipple (Ref. 37) describes the photographic methods now in use. Essentially, the meteor trail is photographed simultaneously from two different camera sites over a base line of about 30 or 40 km. The cameras are aligned to photograph a common volume of sky and there are two cameras at each site. The technique is similar to that shown in Figure 2 for sodium vapor trails.

One of the cameras used by Liller and Whipple (Ref. 38) had an aperture of  $12\frac{1}{4}$  in., a focal length of 8.0 in., and a field view of  $55^\circ$  on the sky. The focal ratio was extremely rapid,  $f/0.65$  optically, and  $f/0.85$  effectively. The second camera at each site was equipped with rotating shutters that broke the meteor trails into segments separated by  $1/60$  second intervals. In this manner, complete data were provided concerning the trajectories, velocities, and decelerations of the incident meteors.

3. Noctilucent Clouds. One of the most direct measurements of high altitude winds has been furnished by the motions of the so-called noctilucent clouds. The composition of these clouds is still uncertain. Mitra (Ref. 39) presents several possibilities. According to one hypothesis they are composed of ice crystals, since they occur in a low temperature region. Another hypothesis suggests that they are due to cosmic dust produced by a volcanic eruption or by the fall of large meteoroids. These clouds form in the warm part of the year, in high latitudes, approximately from the 45th parallel to the Polar circle. The latitude zone of most frequent appearance is around  $55^\circ$  (Ref. 40). The clouds are observed some hours after sunset or before sunrise, being illuminated by the rays of the sun from below the horizon. The mean height of noctilucent clouds is near 82 km, at the height of the temperature minimum of the upper atmosphere which ranges from 74 km to 92 km.

Stormer (Ref. 41) arrived at the heights of these clouds by photographs taken at three sites and the velocities by visual estimates.

### C. RADIO METHODS

1. Chaff. Some winds are measured in the 30-90 km altitude region by means of chaff ejected from rockets. Chaff is usually in small short strips approximately 5 centimeters in length and  $10^{-3}$  cm thick (Ref. 42). The chaff strips are coated with aluminum in order that they can easily be tracked by radar.

The chaff is bound together in cylindrical bundles and placed in the rocket nose cone. When the rocket reaches a specified altitude, the chaff bundles are ejected and the chaff forms a cloud which is tracked by a ground-based radar (see Fig. 3). Smith reports that the initial ejected chaff cloud is cylindrical with its major axis along the rocket trajectory. As the chaff falls, the radar tracks the part of the cloud having maximum concentration. Once the cloud has dispersed, initially, its horizontal movement is interpreted as wind.

2. Meteor Trails. Meteor trails which are generally visible in the altitude region from 110 to 60 km, have furnished much information about atmospheric phenomena at these altitudes. Wind measurements can be obtained from meteors as they enter the atmosphere due to the heavily ionized trail which they leave behind as they burn up. The true wind motion of the air molecules and ions can be observed by means of radio echoes from the drifting meteor trail, whose electron concentration is several orders of magnitude greater than that of the ambient ionosphere (Ref. 43). To determine the wind velocity it is necessary to know (1) the line of sight velocity of the trail to the transmitter-receiver on the ground, and (2) the position of the trail in the atmosphere. The radial component of the wind velocity (see Fig. 4) is established from the difference in frequency between the incident and reflected radio beam due to the Doppler effect. The location of the reflecting ionized trail in space is obtained from the range records (Ref. 44). Greenhow and Neufeld (Ref. 45) obtain the height of the reflecting layers within  $\pm 3$  km by using an empirical curve relating rate of decay time and altitude.

In order to determine the horizontal wind velocity, it is necessary to observe a number of meteors at various azimuth and elevation angles. This is done by directing a beamed aerial alternately in two directions, which are 90 degrees different in azimuth, for a period of several minutes. In this way, average radial wind velocities are obtained and the horizontal components ( $V_1$  and  $V_2$ ) of these are combined to give the resultant wind speed and direction (see Fig. 4). Other similar methods of obtaining wind observations from meteor trails make use of the electronically sweeping antenna pattern obtained by using an array of four vertical antennas spaced about a vertical reflector (Ref. 26) or by using a system of three receiving aerials at the corners of a right triangle (Ref. 46).

3. Radio Fading. Radio fading is one of the most frequent methods used to measure winds in the ionosphere. In the spaced-receiver method, Mitra (Ref. 25), a pulsed transmitter is employed which operates on a frequency range between 2 and 6 Mc/sec. The pulsed beam that is sent out is reflected back when it attempts to penetrate an ionospheric electron layer of sufficient density. The back-scattered signal is received by three aerials located at the vertices of a right triangle (see Fig. 5). The optimum spacing for the receivers is of the order of one wave length.

From the observation times ( $T_A$ ,  $T_B$ ,  $T_C$ ) of similar features of the fading curve records (see Fig. 5) and the distances between the receiver stations, the drift velocity relative to the ground, is readily computed. It follows from simple geometry that the velocity of the ionized cloud drifts is one-half of the ground drift velocity. The height of the particular ionized cloud in the atmosphere is determined by the travel time and frequency of the wave.

4. Sporadic E. A rather frequent electron intensification of a layer,  $\frac{1}{2}$  to 2 km in thickness near 100 km, occurs in the E-region mostly in the summer time. This layer, in which the electron concentration is observed to be as much as twice that in the ambient ionosphere (Ref. 47), is called the sporadic E layer. Wind measurements can be made from the drifting sporadic E



Wallops Island, Virginia, are presented in Figures 6 and 7. Because of the small sample, no statistical analysis is performed and only clues for probable wind flow characteristics are looked for. From these curves the largest variations in speed and direction occur between the altitudes of 90 and 125 km for speed, and 90 and 116 km for direction. The wind speed can change by as much as 128 m/sec in an 8 km altitude change, and 100 m/sec in 3 km; the wind direction backs or veers by as much as 300 degrees in 7 km, and 180 degrees in 1 km. Between 116 and 155 km altitude the directions change very little and are predominantly northerly.

Figure 8 is a replot of the data in Figure 6 in order to show the range of the wind speeds more clearly. Based on available data, the envelope curves connect the lowest and highest wind speeds at the different altitudes; and the intermediate curve connects the wind speeds ranking fifth in magnitude at the different altitudes. The envelope curves are shown as broken lines where the number of cases falls below eight. The greatest ranges of wind speed occur in the 90 to 125 km altitude region. The maximum range and speed, which are respectively 125 m/sec and 148 m/sec, occur at 117 km. The wind speed range is less than 80 m/sec from 127 km to 155 km. The minimum speeds are near 20 m/sec from 85-125 km, and then increase to values near 60 m/sec at 155 km. The maximum wind speeds are near 100-140 m/sec from 90-155 km.

2. Wind Vector Variations. The wind speeds and directions presented in Figures 6 and 7 are shown in Figures 9 and 10 by the months of the year in the form of an aerogram of wind vectors. Also, presented in Figures 9 and 10 are data obtained by sodium vapor trail observations at Eglin Air Force Base, Florida (Ref. 35), at Holloman Air Force Base, New Mexico (Ref. 36), and Wallops Island, Virginia (Ref. 34), and data obtained by chaff observations from Tonopah Test Range, Nevada (Ref. 42).

The wind soundings show rather uniform veering and backing of the wind with altitude. These variations, which are probably due to thermal influences, indicate that there are organized circulations in the 80-200 km region. There are also some sharp changes of the wind velocity with altitude, which may be caused by

ionized clouds by the same technique as in the preceding section with the exception that a higher radio frequency is used in order to penetrate the ambient E layer.

5. Radio-Star Scintillation Method. Of all the methods of measuring wind speeds at extremely high altitudes, the radio-star scintillation method is probably the simplest concept in practical use. Essentially, this method consists of measuring the fluctuations of continuously emitted signals from a radio star. The fluctuations observed are due to the propagation of the signals through drifting ionospheric irregularities. For example, a smooth ionosphere causes the radio waves from the star to undergo a steady refraction. On the other hand, a moving ionosphere containing irregularities or blobs with electron concentrations slightly higher or lower than the surrounding medium, can cause appreciable variations in the refraction of radio-star waves (Ref. 48) and thus produce signal fluctuations. These drifts are measured by three identical interferometers located at the vertices of a right triangle. The technique of measurement is essentially the same as that of radio-fading method except that the signals originate from a star source instead of a ground-based transmitter.

Some of the major difficulties associated with this technique are (1) the height of the irregularities that cause radio-star scintillations is not known, (2) measurements can only be obtained during a few hours at night, and (3) since the signal source does not ordinarily occur overhead, the signal must traverse the atmosphere obliquely.

### III. PRESENTATION AND DISCUSSION OF DATA

#### A. WIND FLOW CHARACTERISTICS

1. Speed and Direction Variations. In the past few years, it has been possible to obtain direct measurements of wind speed and direction above 80 km by ejecting sodium vapor into the atmosphere from rockets. Wind speed and direction curves resulting from the reduction of eight sodium vapor trail observations at

front-like discontinuities and/or markedly sloping anticyclones and cyclones. Moreover, the pronounced daily variation in the wind vector is evidence of migratory anticyclones, cyclones, and thermal variations.

There is evidence, in Figures 9 and 10, for the Winter-to-Summer and Summer-to-Winter transitions in the zonal wind flow for different layers in the 80-200 km region, just as for layers below 80 km. The transition, the associated altitude layers, and times appear to be as follows:

a. Winter-to-Summer transition

(1) From west to east, 70-90 km, between the last half of March and beginning of April.

(2) Ill-defined, 90-110 km

(3) From west to east, 110-160 km, between the last half of April and the first half of May.

b. Summer-to-Winter transition

(1) From east to west, 70-80 km, sometime in October.

(2) Ill-defined, 80-100 km

(3) From east to west, 100-170 km, between the last half of October and the first half of November.

It seems that the transitions in the 110-160 km altitude layer occur later than those in the 70-80 km layer. The layer which is ill-defined with respect to zonal directional change appears to be 10 km higher in Spring than in Autumn.

The wind flow characteristics mentioned in this section are also evident in the mean zonal and meridional time cross sections for the atmospheric region up to 200 km. These cross sections are described in the next section.

### 3. Zonal and Meridional Wind Components Variations.

The monthly zonal (west and east) wind components between 30 and 40 degrees north latitude for the 20-200 km atmospheric layer are presented in Figure 11. Figure 12 shows the meridional (south and north) wind components for the 70-200 km layer. For both the zonal and meridional time cross sections, the wind components above 70 km were obtained from the data presented in Figures 9 and 10. The zonal wind components below 50 km are after Batten (ref. 49). Batten's cross section between 50-70 km was modified slightly by considering chaff and sodium vapor wind data. Isotachs are shown for every 50 m/sec. A considerable amount of smoothing necessarily went into the analysis above 70 km, since the data samples were limited. Inference of the expected wind flow above 100 km in the wintertime is indicated by broken isotachs. These cross sections are to be regarded as first estimates of the monthly wind flow in the 80-200 km region, which can be taken as applicable to the Cape Canaveral, Florida, area.

The mean zonal winds are predominately westerly from the surface up to about 90 km during the winter months. The maximum mean westerly wind flow in this region is near 100 m/sec, and occurs during the latter part of January around 70 km. There appears to be a small band of easterlies between 90 and 110 km with magnitudes less than 50 m/sec. From 110 up to 200 km, the zonal winds are, again, predominately westerly. There seem to be two wind maxima in this region. One maximum occurs during February and March around 120 km, while the other occurs during January and February, possibly near 180 km. Both of the centers have magnitudes above 100 m/sec.

For the summer months, the zonal winds are predominately easterly from the surface up to about 80 km. The maximum mean flow of about 60 m/sec occurs during the early part of July around 60 km. There is a small band of westerlies above this region extending from 80 to 110 km. The maximum wind speed magnitude near 100 km is above 50 m/sec. Above 110 km, the wind again changes to easterlies. These easterlies extend to 200 km. The winds in this region appear to have three areas of maximum concentration. Two of these areas are near 120 km, and occur during the months of May, June and August. Both

areas have magnitudes above 100 m/sec. The other area of maximum wind flow above 100 m/sec near 170 km altitude slopes from 180 km during the latter part of July to 160 km during the middle of September.

Figure 11 indicates that the zonal wind between 70 and 80 km altitude changes from westerly in the winter to easterly in the summer. Wind speeds for the winter in this region appear to be about twice as large as those for the summer. Above 80 km, although the zonal wind direction appears to be opposite in winter and summer in the 80-110 km, in the 110-140 km, and in the 140-200 km layers, it is difficult to compare the wind speeds for summer and winter because of gaps in the data. The transition times for the reversal of the zonal wind flow direction for the layers above 70 km lie in the periods indicated in Section 2 above.

The mean meridional wind flow pattern below 70 km is not as well defined as the zonal. The wind magnitude in this region for Cape Canaveral, Florida, is generally less than 10 m/sec (Ref. 50). In the wintertime above 70 km the mean wind is northerly between 80 and 100 km, and has a maximum magnitude of more than 50 m/sec. A small band of southerly winds is apparently present between 105 and 115 km. Wind magnitudes for this region can attain values greater than 50 m/sec. The meridional wind direction between 115 km and 200 km appears to be predominantly northerly with magnitudes as high as 150 m/sec in individual cases (Ref. 51).

During the summer months, the winds between 70 and 140 km altitude alternate between southerly and northerly and become predominantly northerly above 140 km. The wind speeds are generally less than 50 m/sec below 140 km except in August, when a wind of 150 m/sec was observed near 120 km. Northerly winds of this magnitude are also observed above 140 km.

The large meridional wind speeds, particularly above 140 km for the 20-40 latitude region, seem to indicate that the wind vector backs or veers without much diminution of magnitude in the Winter-to-Summer and Summer-to-Winter transitions of zonal direction. From the very limited data now available for the

140-200 km region, the north component seems to maintain itself through spring and only reverses sometime between the last half of August and the first half of September. The autumn east-west reversal in this region occurs at a later time. The south component is evident to at least December.

4. Additional Summer and Winter Ionospheric Winds in the 80-400 km Region. An extensive literature survey was made in an effort to include as much data as possible on the winds above 80 km. Figure 13 presents a sample of the winds from that survey (Ref. 4-28). There are a few winds shown just below 90 km which are the results of meteor trail observations; otherwise, the winds shown were measured by ionospheric drift techniques. The winds are plotted for the summer and winter as a function of altitude and latitude. In most instances, a specific altitude was not available, and the winds were plotted either at the midpoint of the altitude interval or at the assumed midpoint of a particular layer of the ionosphere. The E, F, and F<sub>2</sub> ionospheric layers are indicated on the right ordinate axis of the figure. No data were obtained for the F<sub>1</sub> layer. The altitudes of the peak electron concentrations in these layers, particularly in the case of the F<sub>2</sub> layer, are actually not clearly fixed since the peak concentrations and their levels vary diurnally, seasonally, latitudinally, and with the sunspot number. In cases where the observations were recorded for at least one year, and the authors did not make a distinction between summer and winter, the winds have been plotted the same for both seasons. Two flags originating from one point indicate that a change in the direction occurs sometime during the day. Additional information can be found in the legend of Figure 13. A distinct wind flow characteristic shown by this figure is that the winds above 200 km are markedly zonal with a diurnal change of direction.

Millman (Ref. 52) summarized the general characteristics of about 50 long-duration meteor trains. Several distinct types of differential wind currents were found between 80 and 100 km of altitude. Typical examples were the S, Z, and C forms, a square form, trains with one sharp bend, those showing evidence of a narrow jet stream, and those showing generally irregular diffuse patches. The meteor train drifts were predominantly horizontal with normal speeds of about 50 m/sec. From 40 selected

trains, Millman found that the average spacing between major wind currents moving in opposite directions was 8.3 km along the meteor path. This corresponds to a vertical height difference in the atmosphere of about 6 km. The average differential velocity between these major wind currents was determined to be 30 m/sec, i. e., a shear of  $0.005 \text{ sec}^{-1}$ .

Millman also discusses noctilucent clouds and states that the motion of clouds tends to be mostly toward the west. Velocities have been measured in the range 30 to 70 m/sec with an average velocity of about 50 m/sec. On occasions, however, he has noted velocities between 100 and 200 m/sec. The height of these noctilucent clouds is usually around 80 km. Noctilucent clouds normally exhibit elements of a regular structure, sometimes taking the form of a series of long parallel wave crests with a spacing of 9 km between successive crests. The crests are sometimes crossed by a second system of parallel lines at right angles to the first. Noctilucent clouds are observed at high latitudes.

The use of radio methods has produced evidence of horizontal drifts or movements in the E and F regions of the ionosphere. It is still questionable as to what part of these movements are due to pressure gradient forces and what part due to geomagnetic and electromagnetic fields at very high altitudes. It is also questionable whether the movements observed are actual winds, that is, movements of air particles.

From a study of "winds" in the F-region of the ionosphere, Singh and Khastgir (Ref. 12) found that a sudden reversal in the direction of the wind occurred around midnight. Such reversals were usually followed by turbulence. Irregularities of the ionosphere were observed, and in some cases attributed to a "single" ion cloud movement. Quasi-periodic, regular periodic and random patterns of drift were recorded.

Ratcliffe (Ref. 53) states that horizontal gradients of electron density are greatest at sunrise. The drifts in the F-region are predominantly zonal. Below about 400 km at  $50^{\circ}$  N latitude, they are toward the east by day and toward the west by night, and have magnitudes of about 50 m/sec. Near the magnetic equator the direction of drift is reversed; it is toward the west by day and the

east by night. The magnitude of the F-region drift is greater during times of increased magnetic activity. The probability of a reversal of direction near 0200 hours local time increases with an increase in magnetic activity.

5. Extreme Winds. The literature was also examined for extreme wind speeds. The estimated maximum wind speed that occurs in the atmosphere above 80 km is illustrated in Figure 14. This estimate was based on values obtained from the literature and on the data presented in the previous figures. A sample computed estimate utilizing the data obtained from sodium vapor trails was found to be in good agreement with this profile for the altitude region between 100 and 130 km. The profile presented in this figure should be considered as an envelope. The maximum values will increase (decrease) according to an increase (decrease) in solar activity, especially, above 150 km of altitude, but are not expected to exceed the profile values. However, it should be mentioned that at least four authors have reported observations of movements in the ionosphere exceeding the profile values. Yerofeyev (Ref. 16) reported 490 m/sec as a maximum in the 200-300 km region, Briggs and Spencer (Ref. 54) reported 1000 m/sec at 300 km and 750 m/sec in the F-region, and Chapman (Ref. 55) reported 500 m/sec in the E-region. These radio drift observations were recorded for brief periods during magnetic storms, and it is quite probable that these movements are not true wind movements of air particles.

6. Wind Shear and Turbulence. Wind shears were calculated from the wind speed and direction data in Figures 6 and 7 for height increments of 500, 1000, 3000, and 5000 m using the following equation:

$$S = \frac{[(V_n)^2 + (V_{n-1})^2 - (2)(V_n)(V_{n-1})\cos(\theta_n - \theta_{n-1})]^{1/2}}{h_n - h_{n-1}},$$

where S represents the wind shear; V, the wind speed;  $\theta$ , the wind direction; and h, the height. The subscripts n and n-1 correspond to the top and bottom altitudes, respectively, of each layer. The



calculated values were plotted at the midpoints of the various layers in Figures 15-18. For the 500 m layers in Figure 15, shear values were plotted every 500 meters of altitude; whereas, for the 1000, 3000, and 5000 m layers in Figures 16-18 shear values were plotted for every 1000 meters of altitude. It should also be noted that the abscissa scales for the 3000 and 5000 m shears are twice those for the 500 and 1000 m shears. The envelope curves in these figures connect the lowest and highest wind shears at the different altitudes; the intermediate curve for each of the figures connects the wind shears ranking fifth in magnitude at the different altitudes. The envelope curves are shown as broken lines where the number of cases falls below eight.

From Figures 15 through 18, it is quite apparent that the wind shears with altitude are large between 85 and 125 km with peak values occurring between 95 and 110 km. The highest maximum wind shears occur near 100 km with maximum values decreasing above and below this altitude. The peak shear values near 100 km for the 500, 1000, 3000, and 5000 m layers were, respectively, 0.131, 0.086, 0.053, and  $0.035 \text{ sec}^{-1}$ . Above 125 km, the wind shears become quite small, of the order of  $0.005 \text{ sec}^{-1}$ , with only a little variation with altitude. The minimum values in Figures 15-18 are near zero. A close inspection of the data has disclosed that the maximum wind shears, for all height increments concerned, occur during the evening twilight hours between 95 and 120 km. This limited data sample indicates that wind shears are probably larger in the daytime than at night. No comparison between summer and winter can be made here because the observations were obtained only during spring and autumn.

Only a small percentage of the literature mentions the wind shear and turbulence in the ionosphere. Greenhow and Neufeld (Ref. 27), using the radio echo technique to investigate meteor trains between 80 and 100 km, have found the median value of the turbulent wind shear in this region to be 10 m/sec/km with a maximum near 140 m/sec/km. The data show that the rms turbulent velocity does not vary significantly with the gradient of wind, with height, or with the mean wind speed. They found no significant difference between the turbulent velocities observed during day and night time. The large turbulence at heights between 80 and 100 km

was found to be distinctly anisotropic. The vertical scale of the largest eddies was determined to be approximately 6 km; the horizontal scale of these eddies is of the order of 150 km. The lower limit to the scale for the smallest eddies was calculated to be 17 m.

Elford and Robertson (Ref. 46), by use of radio echoes to observe meteor trains, found a positive wind gradient of 3.6 m/sec/km for a small range of heights centered around 95 km of altitude. These results were obtained by utilizing a Fourier analysis which gave a comparison of the amplitudes of the hourly wind vectors for the months of November and December. Elford (Ref. 28), after making further studies, established that the average wind gradient in December was +2.3 m/sec/km, and in June - 3.3 m/sec/km.

By using widely spaced receiving stations and observing ionospheric drifts in the altitude region between 180 and 250 km, Thomas (Ref. 6), found a mean gradient of about 1 m/sec/km for a sample of fifty measurements distributed over both summer and winter months. His figures also suggested that over the altitude range considered (180-250 km), there is a larger gradient of velocity in winter than in summer.

#### SECTION IV. CONCLUSIONS

Although it is realized that the wind information in the 80-400 km ionospheric region of the atmosphere is quite limited, it is nevertheless necessary from the point of view of determining input data for launch vehicle and spacecraft design and performance studies to present the available wind data, to interpret it, and to draw some tentative conclusions of the wind flow characteristics. The following points are made:

- (1) Up to about 200 km the largest variations in wind speed and direction with altitude are between 90 and 125 km. The wind speed can change by as much as 128 m/sec in 8 km altitude change, and 100 m/sec in 3 km; the wind direction backs or veers

by as much as 300 degrees in 7 km and 180 degrees in 1 km. Above about 125 km, the directions change very little with altitude. Above about 200-250 km, based on ionospheric drift measurements, the winds seem to be markedly zonal with a diurnal change of direction.

(2) The probable maximum wind speed increases in steps from near 230 m/sec at 80 km to 500 m/sec at 400 km.

(3) In the 80 to 200 km altitude region the highest wind shears with altitude are between 85 and 125 km with peak values occurring between 95 to 110 km. The largest maximum wind shears occur near 100 km with maximum values decreasing above and below this altitude. The peak shear values near 100 km calculated for the 500, 1000, 3000, and 5000 m  $\Delta h$  layers were, respectively, 0.131, 0.086, 0.053, and 0.035  $\text{sec}^{-1}$ . Above 125 km to at least 200 km it appears that the wind shears with altitude are quite small, being in the order of 0.005  $\text{sec}^{-1}$ . There is evidence, too, that the wind shears to at least 250 km are even smaller.

(4) Judging from the gradual veering or backing of the wind vector with altitude, there appears to be organized circulation in the 80-200 km region. Moreover, the marked daily variation in the wind vector is evidence of migratory anticyclones and cyclones. Also evident are some abrupt changes of the wind velocity with altitude, which may be caused by front-like discontinuities and/or markedly sloping anticyclones and cyclones.

(5) There is evidence of transition in the zonal direction flow during spring and autumn in the 70-80 km and 110-160 km regions. The 80-110 km region is ill-defined in this respect. From about 140 to 200 km it appears that the wind vector veers or backs through these transitional periods without much diminution of magnitude.

(6) A monthly mean zonal cross section from 20 to 200 km for the 30-40 degree latitude belt shows:

(a) In winter, a small band of easterlies (less than 50 m/sec maximum) between 90 and 110 km with westerlies predominantly in the rest of the 80-200 km region.

(b) Besides the westerly wind maximum (near 100 m/sec) around 70 km, a westerly wind maximum (more than 100 m/sec) near 120 km and another westerly wind maximum (more than 100 m/sec) near 180 km.

(c) In summer, a small band of westerlies (more than 50 m/sec) between 80 and 110 km with easterlies in the 110-200 km region.

(d) Besides the easterly wind maximum (more than 60 m/sec) near 60 km an easterly maximum (more than 100 m/sec) near 120 km during May-June, another easterly maximum (more than 100 m/sec) near 120 km in August, and another easterly maximum (more than 100 m/sec) near 170 km also in August.

(7) A monthly mean meridional cross section from 70-200 km for the 30-40 degree latitude belt shows:

(a) In winter, a small band of southerly winds (more than 50 m/sec maximum) between 105 and 115 km.

(b) In winter, northerly winds (more than 50 m/sec maximum) between 80 and 100 km and again predominantly northerly (more than 100 m/sec maximum) from 115 to 200 km with magnitudes as high as 150 m/sec in individual cases.

(c) In summer, alternating southerly and northerly wind cells between 70 and 140 km with mean maximum speeds generally less than 50 m/sec although in individual cases with speeds of the order of 150 m/sec near 120 km in August.

(d) In summer, predominantly northerly (more than 100 m/sec maximum) above 140 km with speeds of the order of 150 m/sec in individual cases.

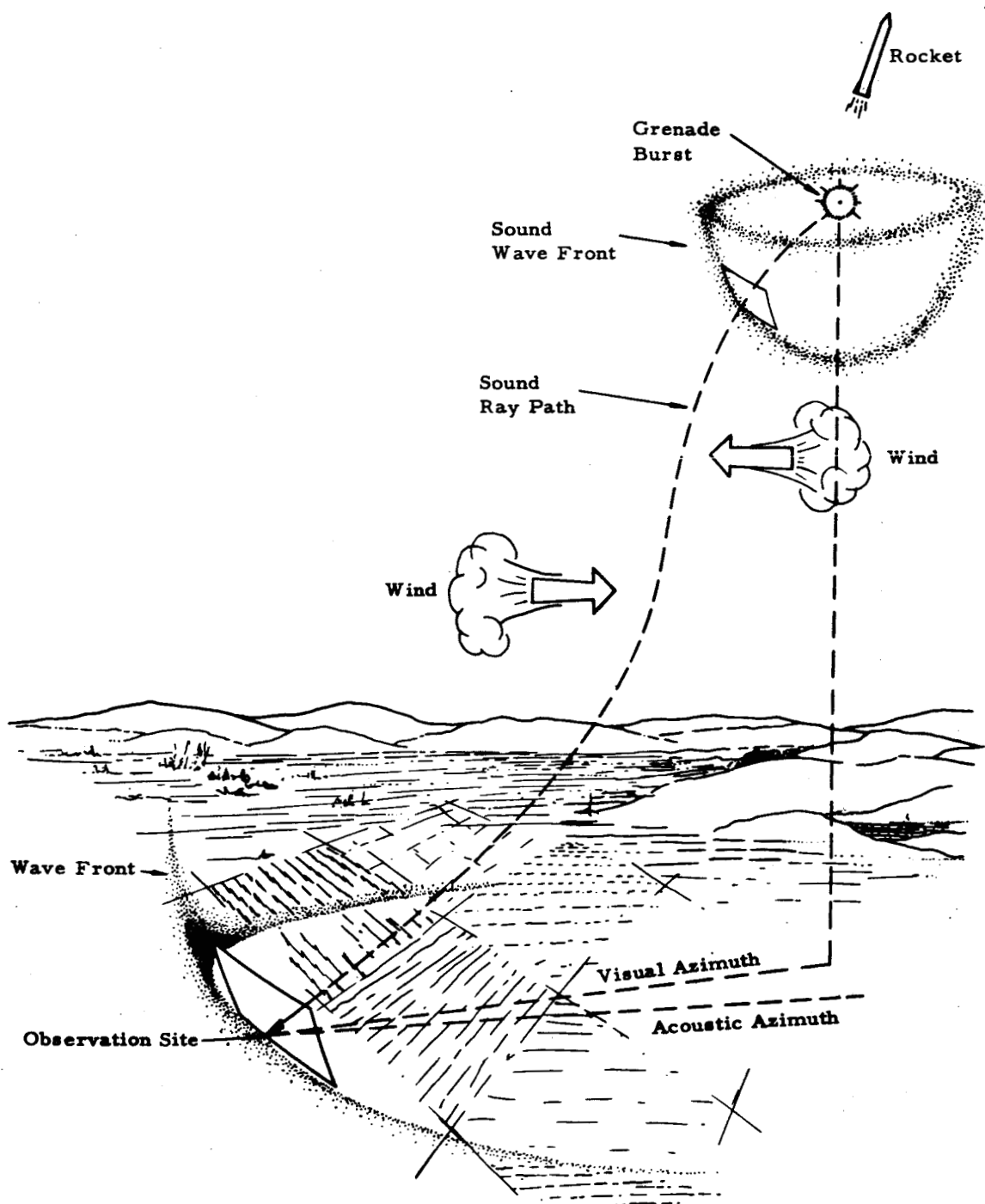


FIG. 1. ROCKET-GRENADE TECHNIQUE OF MEASURING WINDS

MTP-AERO-62-49

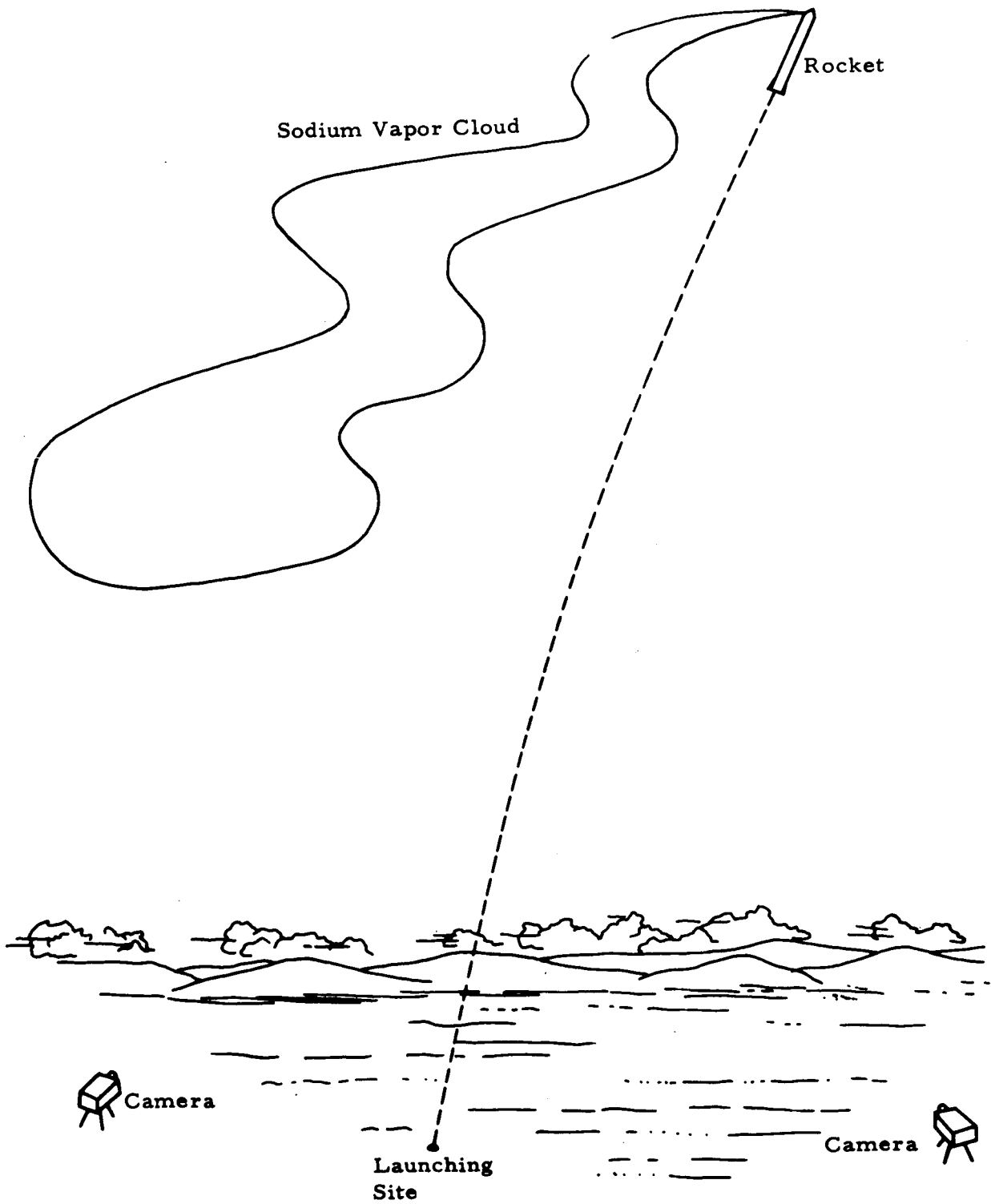


FIG. 2. SODIUM VAPOR TECHNIQUE OF MEASURING WINDS

MTP-AERO-62-49

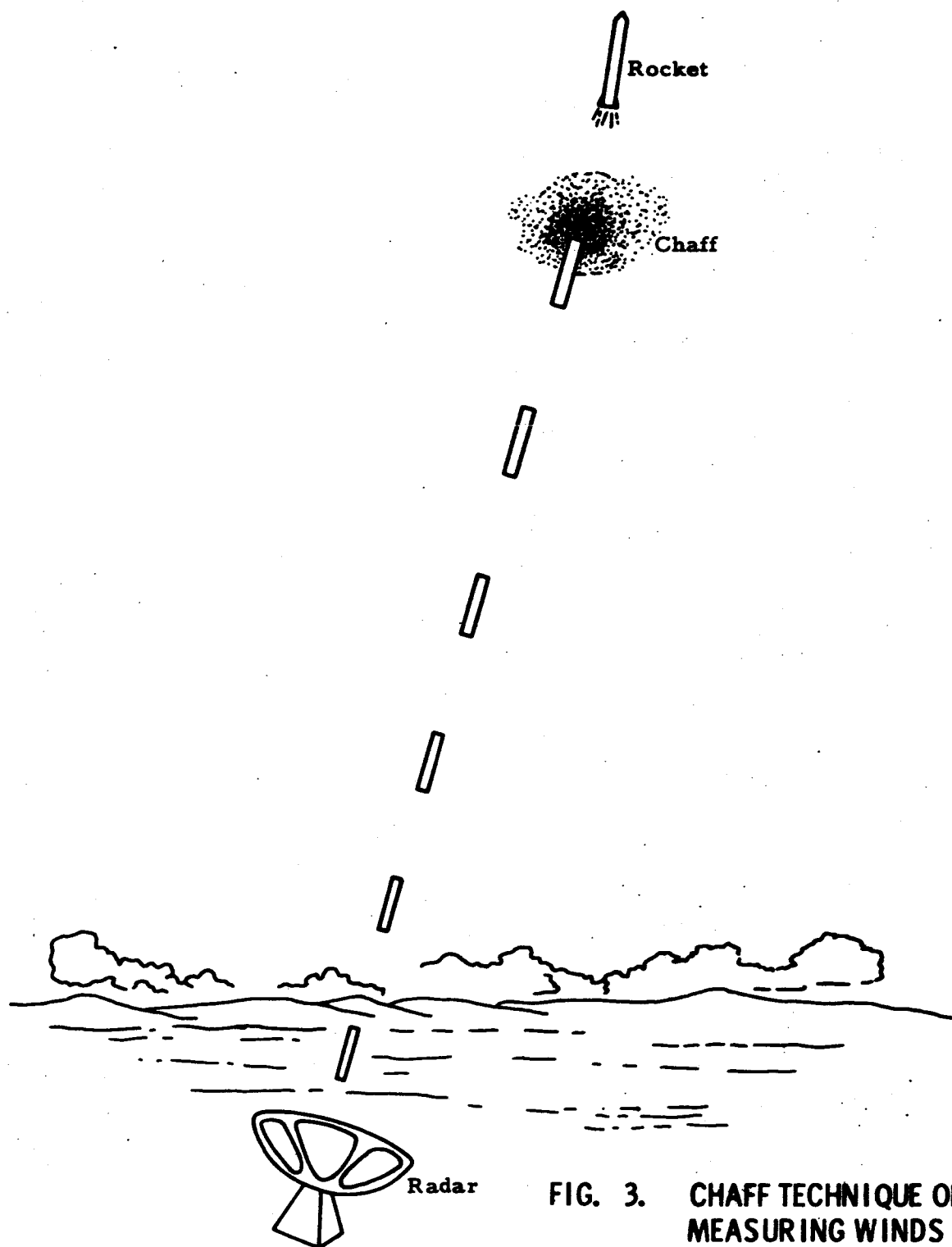


FIG. 3. CHAFF TECHNIQUE OF MEASURING WINDS

MTP-AERO-62-49

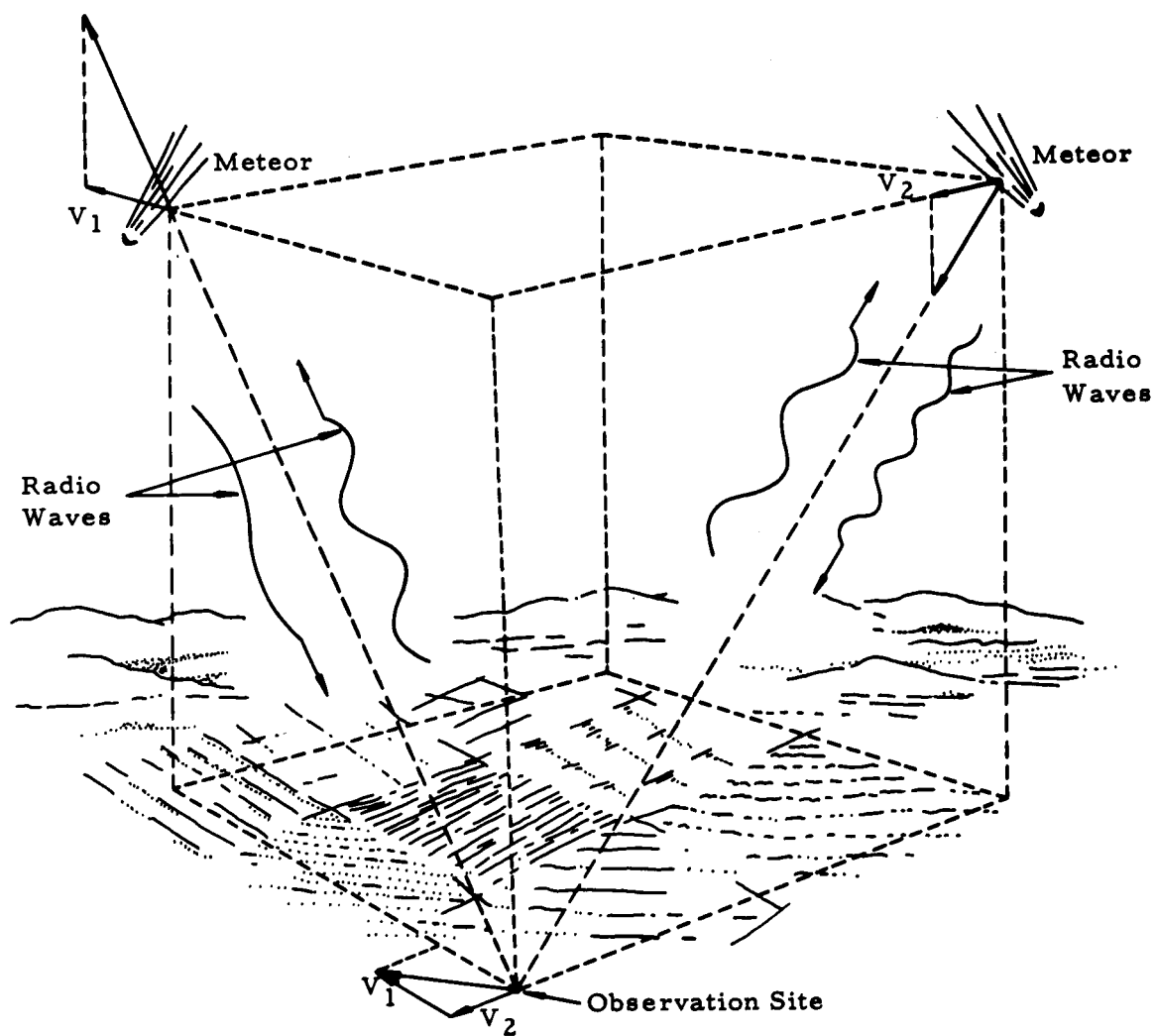


FIG. 4. METEOR TRAIL TECHNIQUE OF MEASURING WINDS

MTP-AERO-62-49



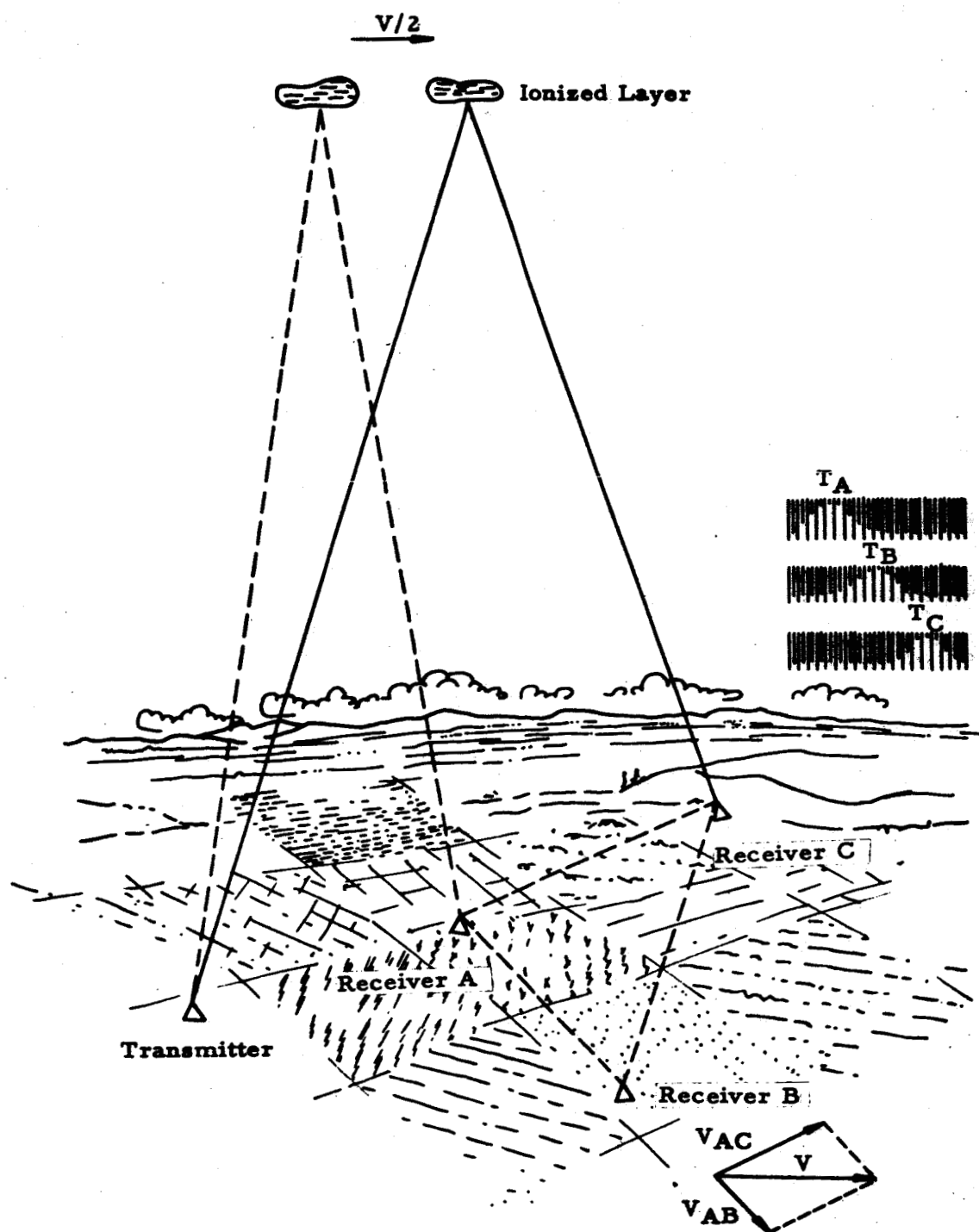


FIG. 5. RADIO-FADING TECHNIQUE OF MEASURING WINDS

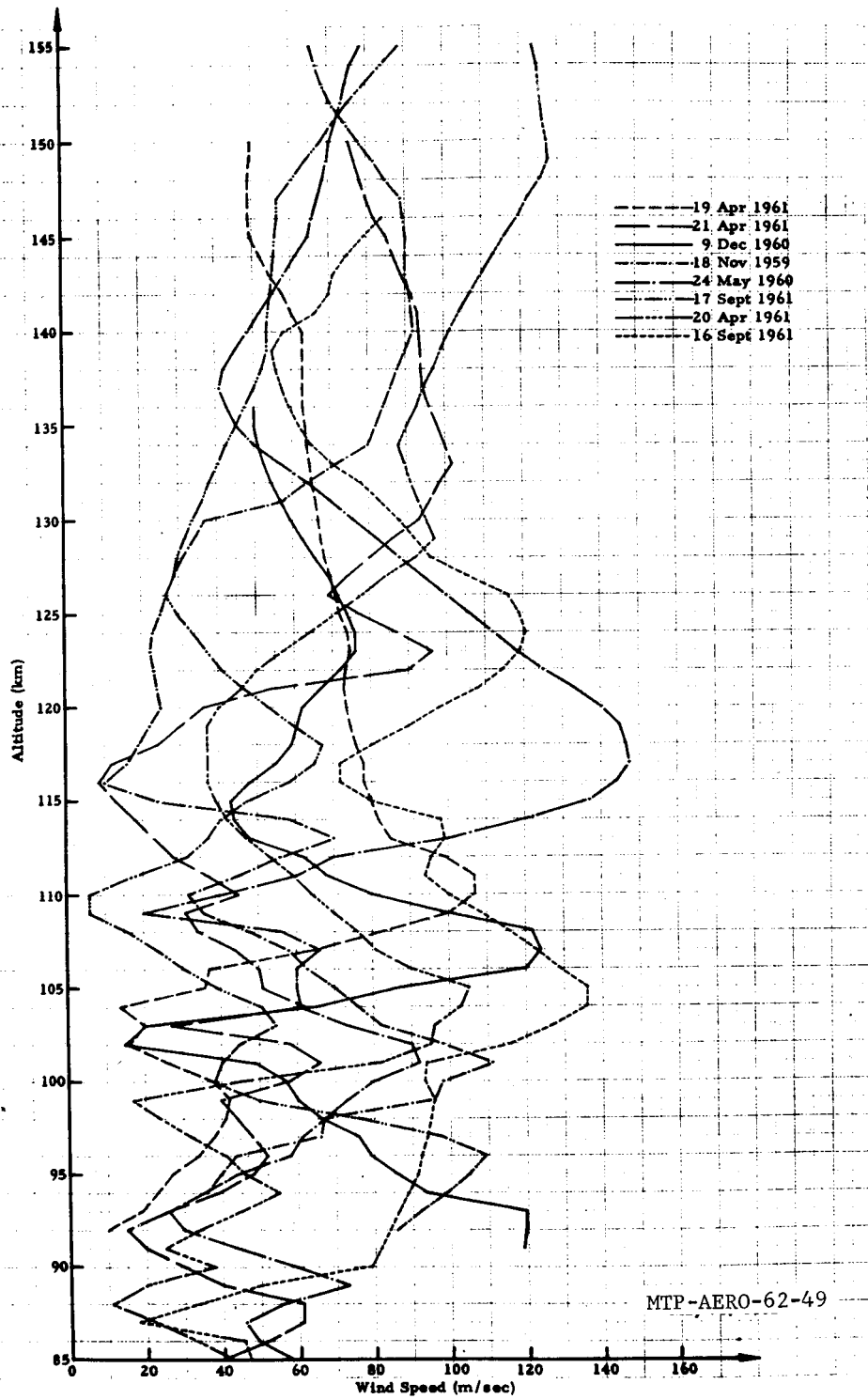


FIG. 6. WIND SPEED CURVES OBTAINED FROM SODIUM VAPOR TRAIL MEASUREMENTS AT WALLOPS ISLAND, VIRGINIA

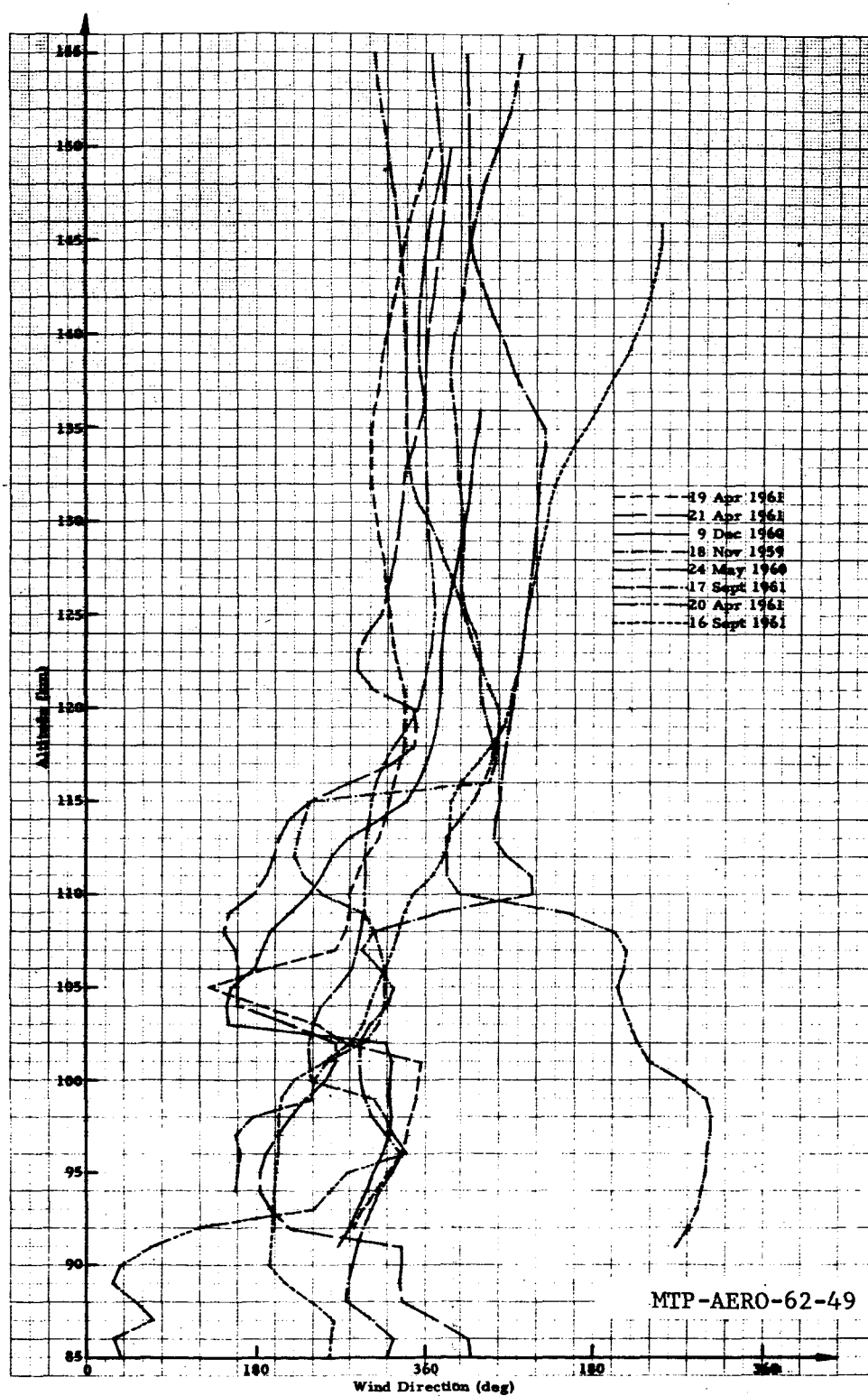


FIG. 7. WIND DIRECTION CURVES OBTAINED FROM SODIUM VAPOR TRAIL MEASUREMENTS AT WALLOPS ISLAND, VIRGINIA

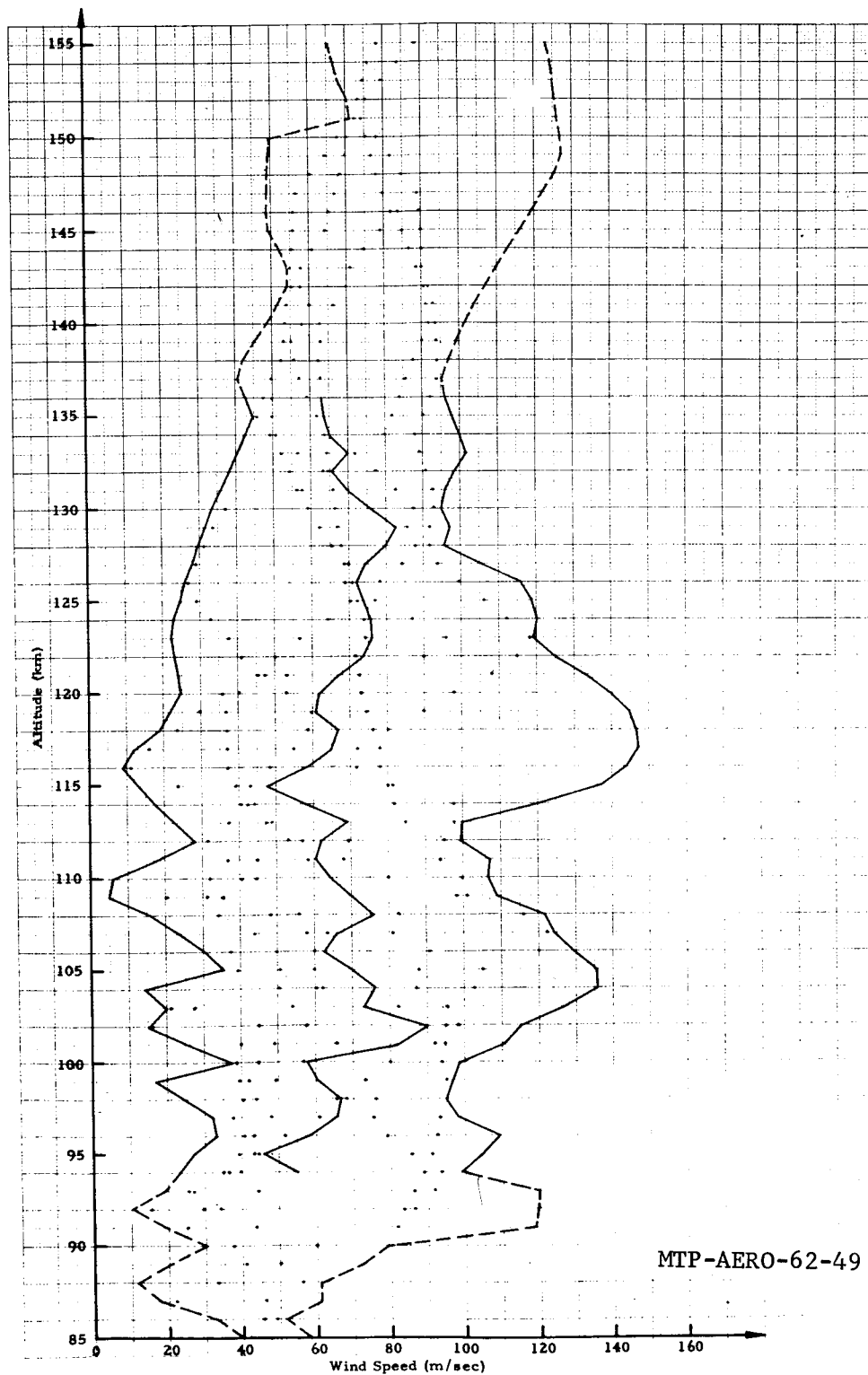
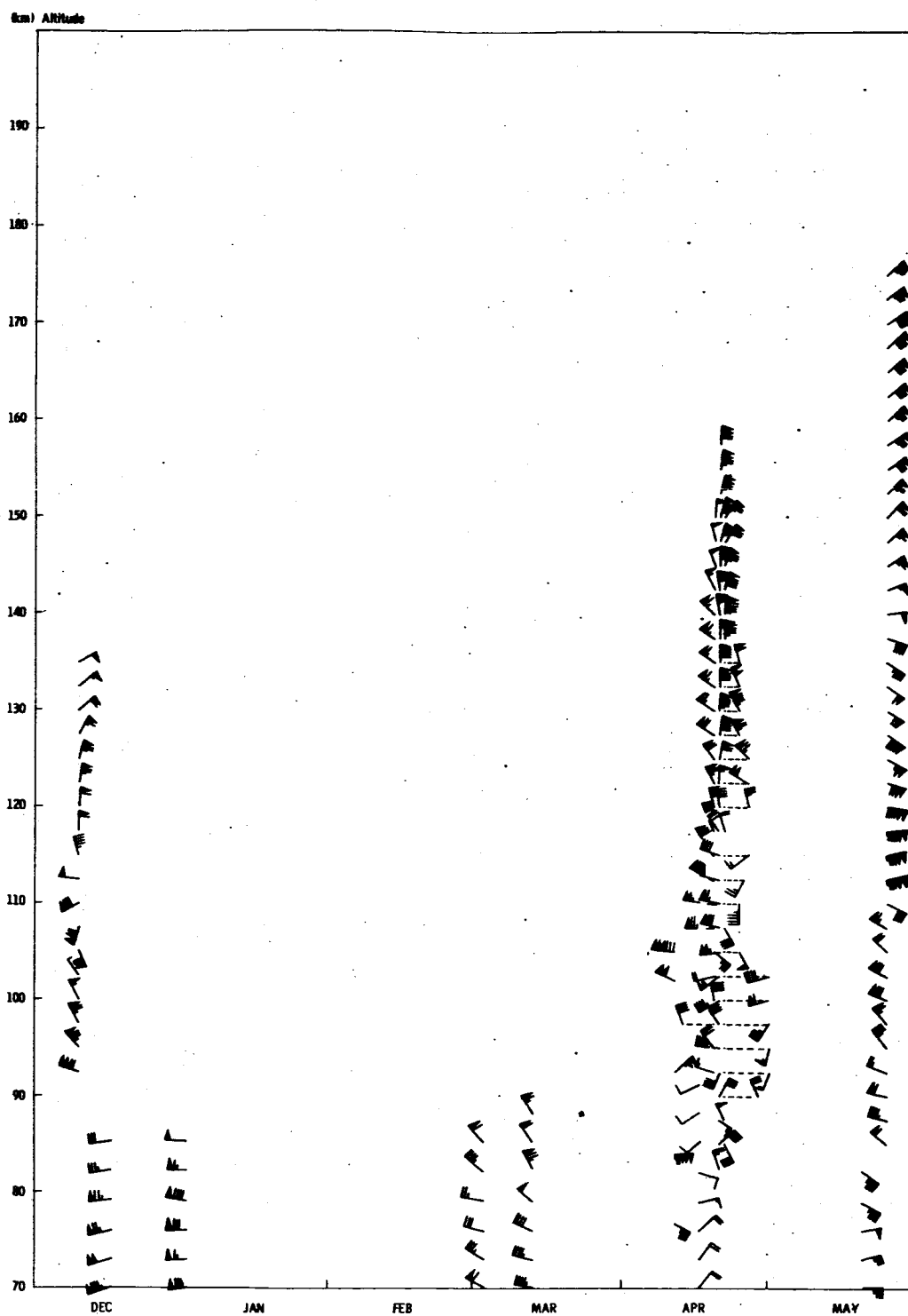
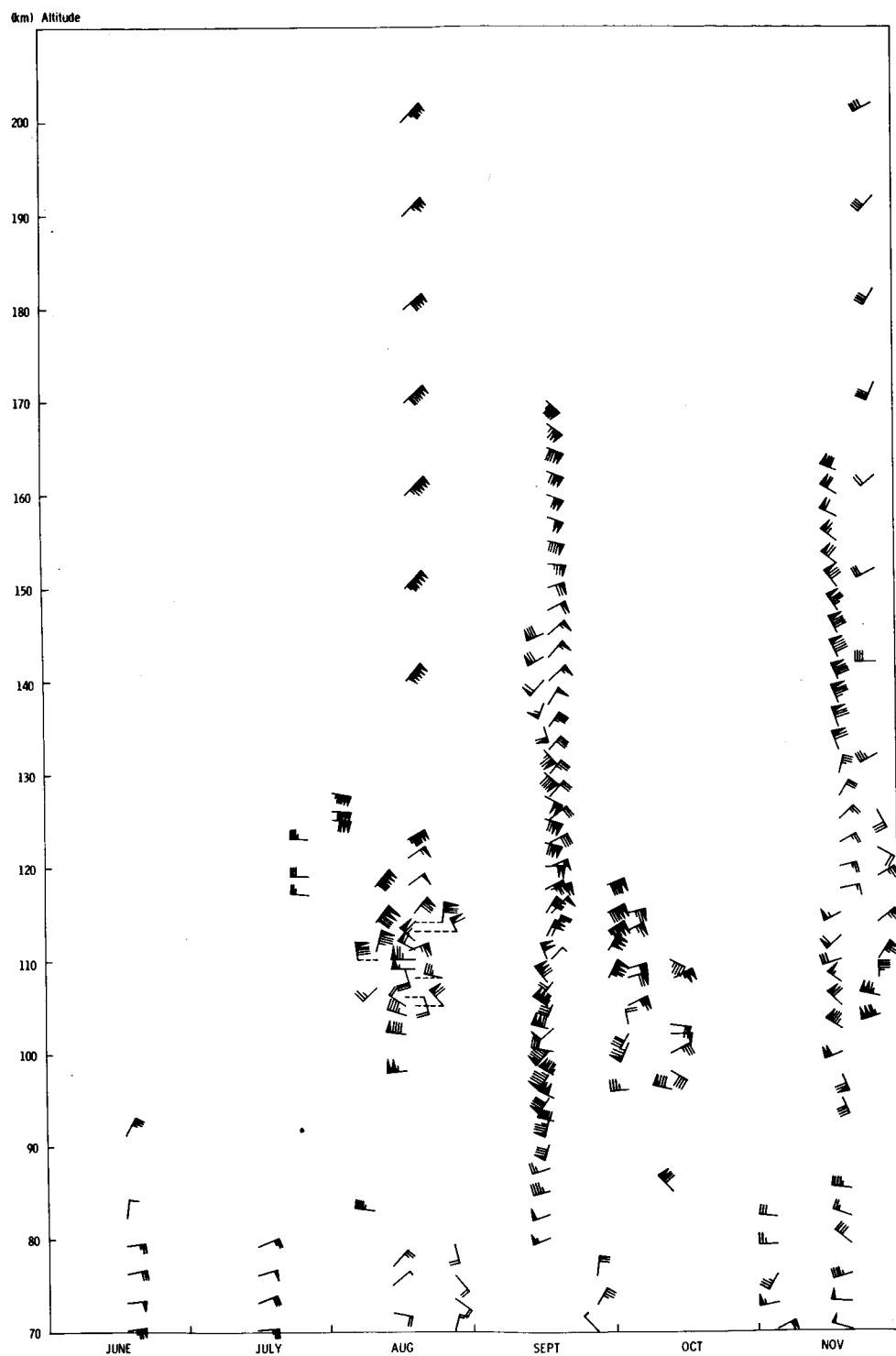


FIG. 8. WIND SPEED ENVELOPES OBTAINED FROM SODIUM VAPOR TRAIL MEASUREMENTS AT WALLOPS ISLAND, VIRGINIA



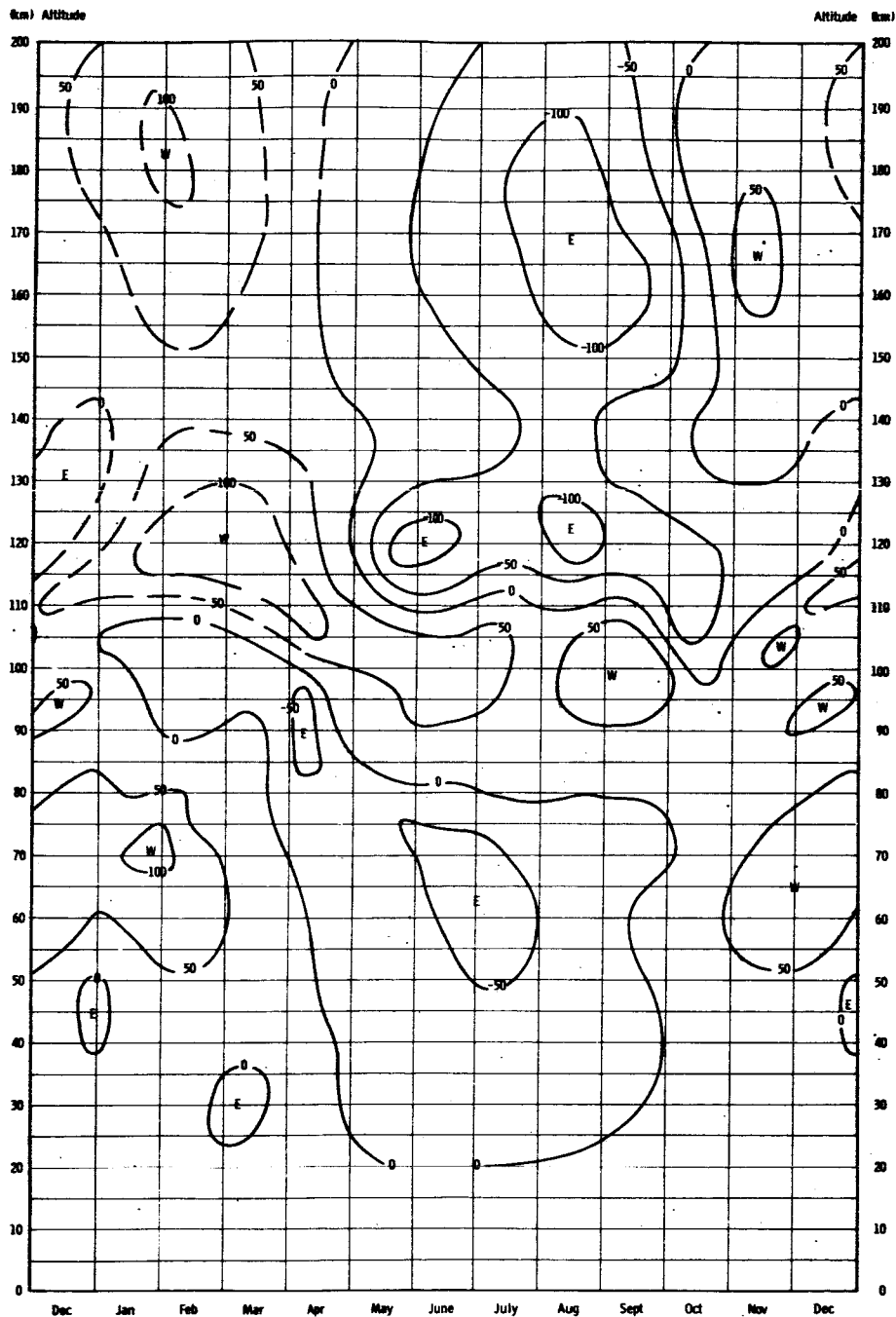
MTP-AERO-62-49

FIG. 9. AEROGRAM OF WIND VECTORS OBTAINED FROM SODIUM VAPOR TRAIL (Wallops Island, VA.; Holloman AFB, N.M.; Eglin AFB, FLA.) AND CHAFF (Tonopah, Nev.) measurements



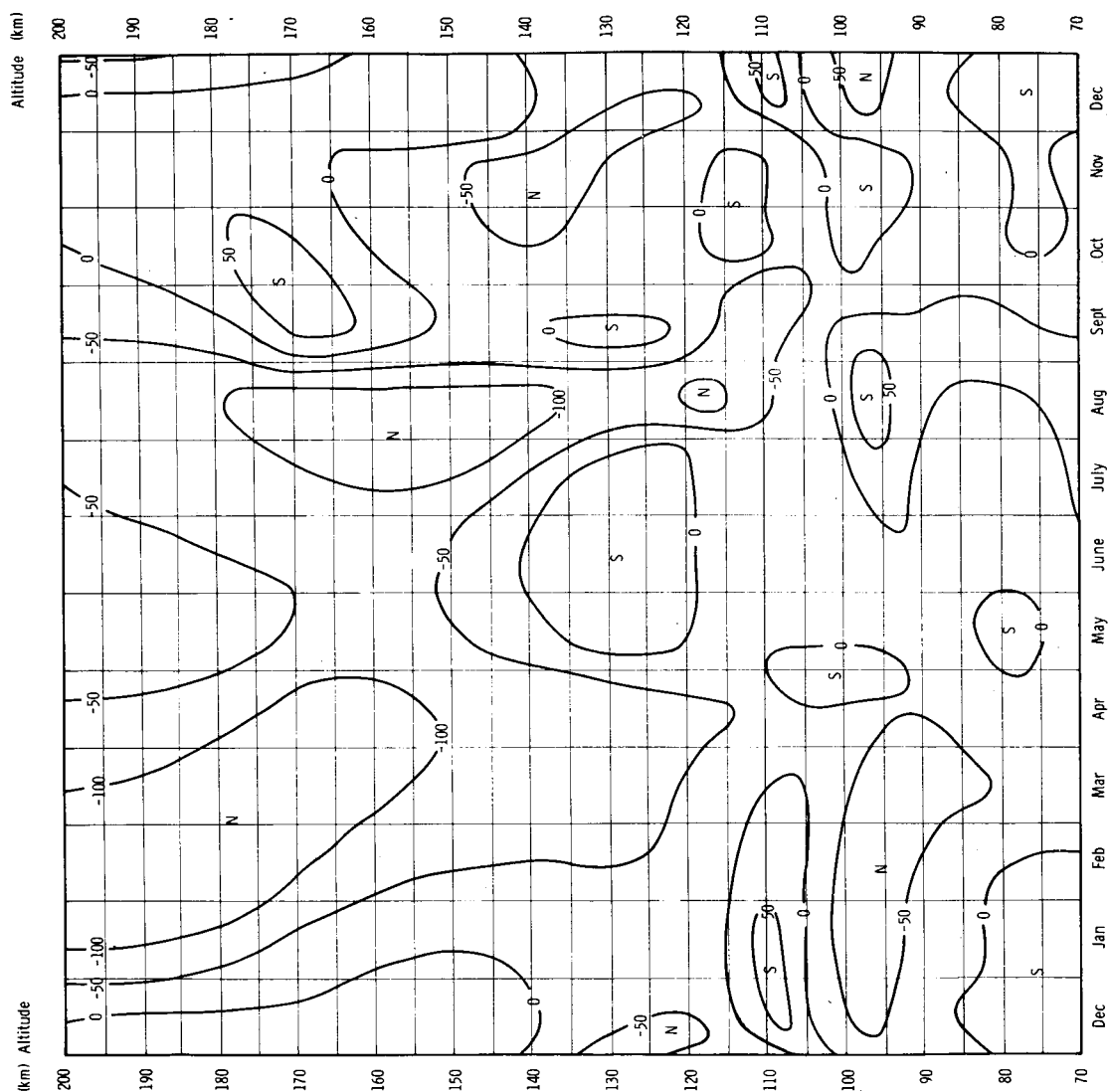
MTP-AERO-62-49

FIG. 10. AEROGAM OF WIND VECTORS OBTAINED FROM SODIUM VAPOR TRAIL (WALLOPS ISLAND, VA.; HOLLAMAN AFB, N.M.; EGLIN AFB, FLA.) AND CHAFF (TONOPAH, NEV.) MEASUREMENTS



MTP-AERO-62-49

Fig. 11. Mean Zonal Wind Cross Section for the 30°-40° North Latitude Belt



MTP-AERO-62-49

Fig. 12. Mean Meridional Wind Cross Section for the 30°-40° North Latitude Belt





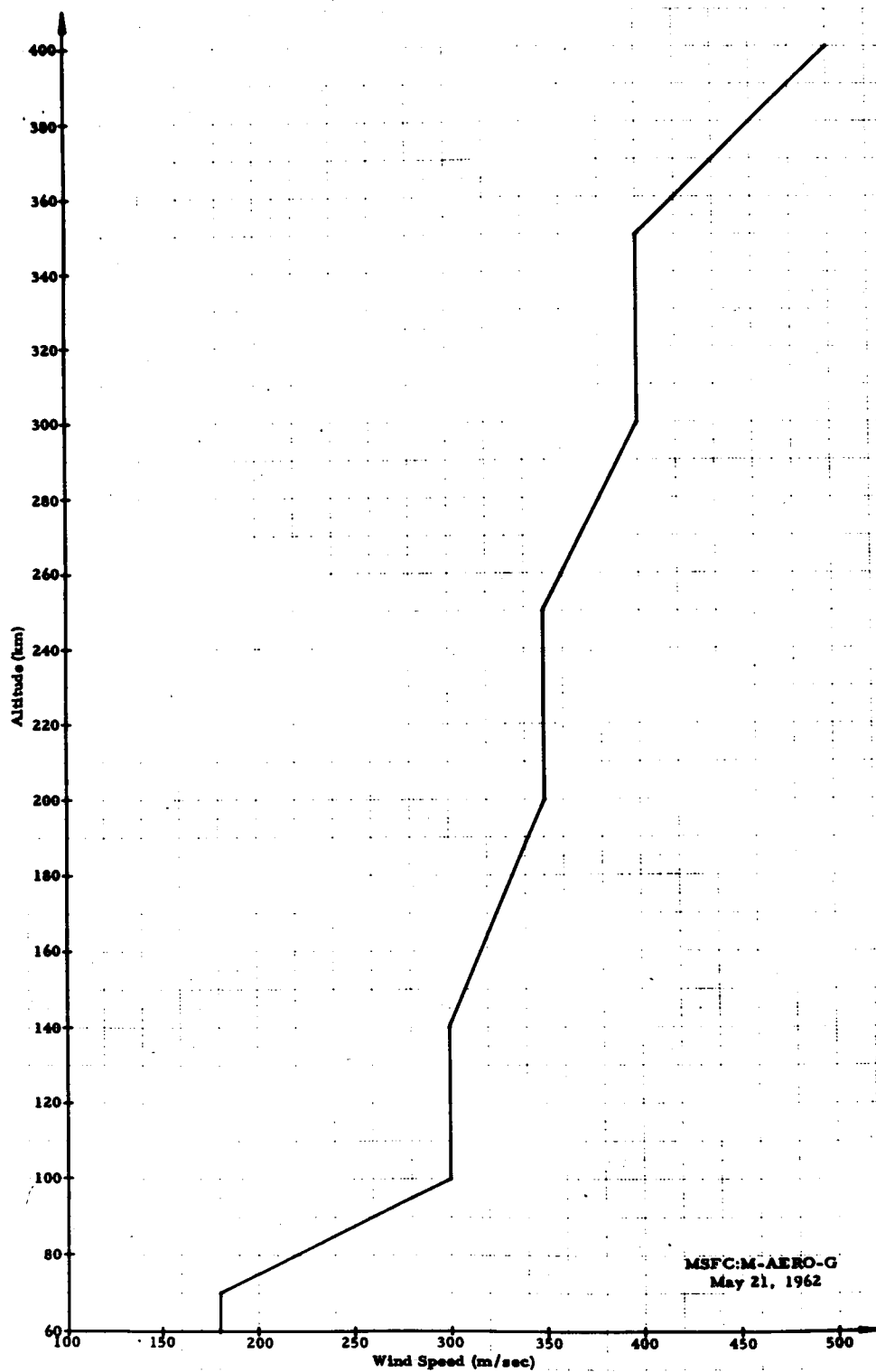


FIG. 14. PROBABLE MAXIMUM WIND SPEED ENVELOPE FROM 60 TO 400 km

MTP-AERO-62-49

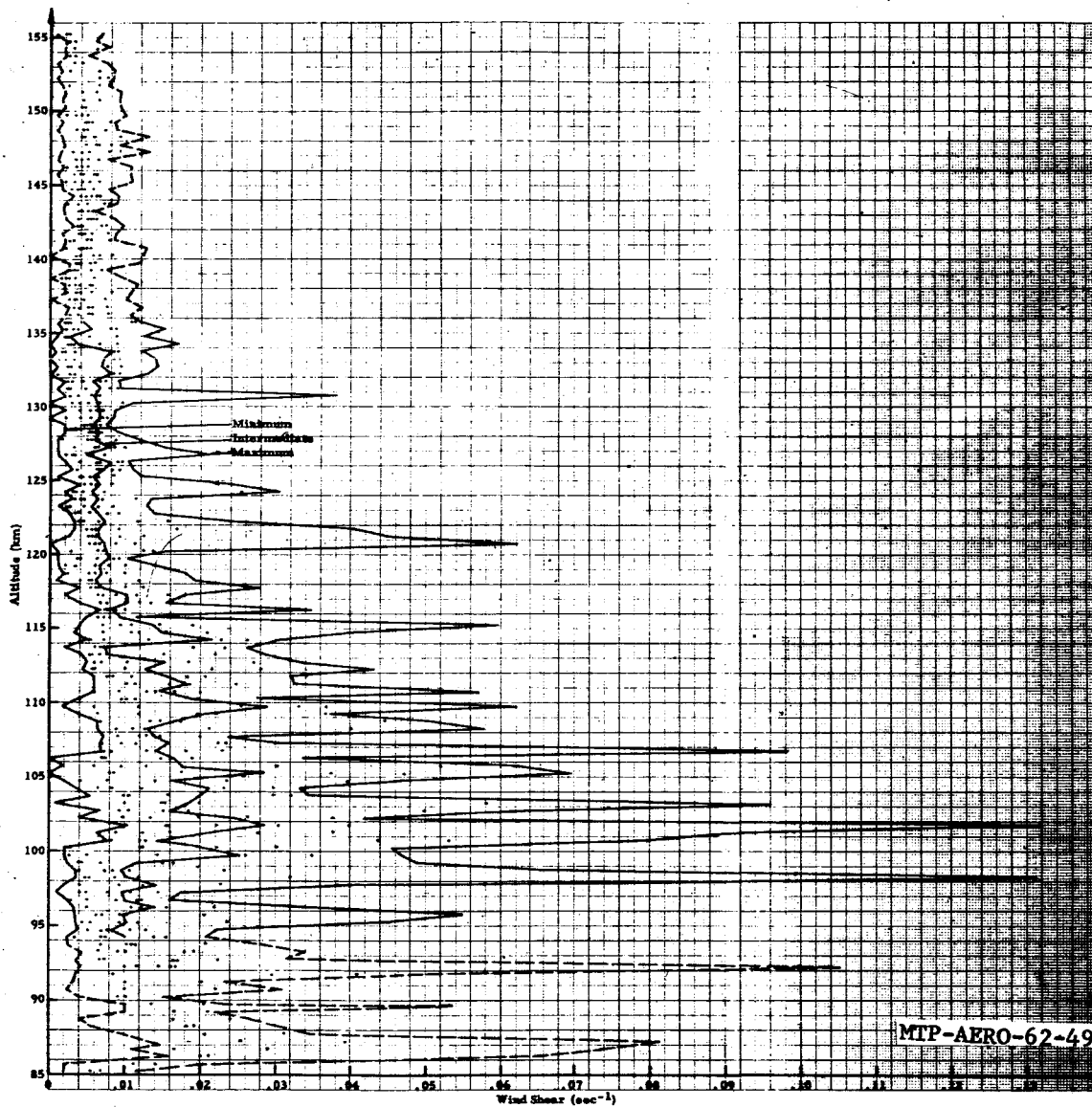


FIG. 15. WIND SHEAR ENVELOPES OBTAINED FROM SODIUM VAPOR TRAIL MEASUREMENTS AT WALLOPS ISLAND, VIRGINIA FOR 500 m ALTITUDE LAYERS (4h)

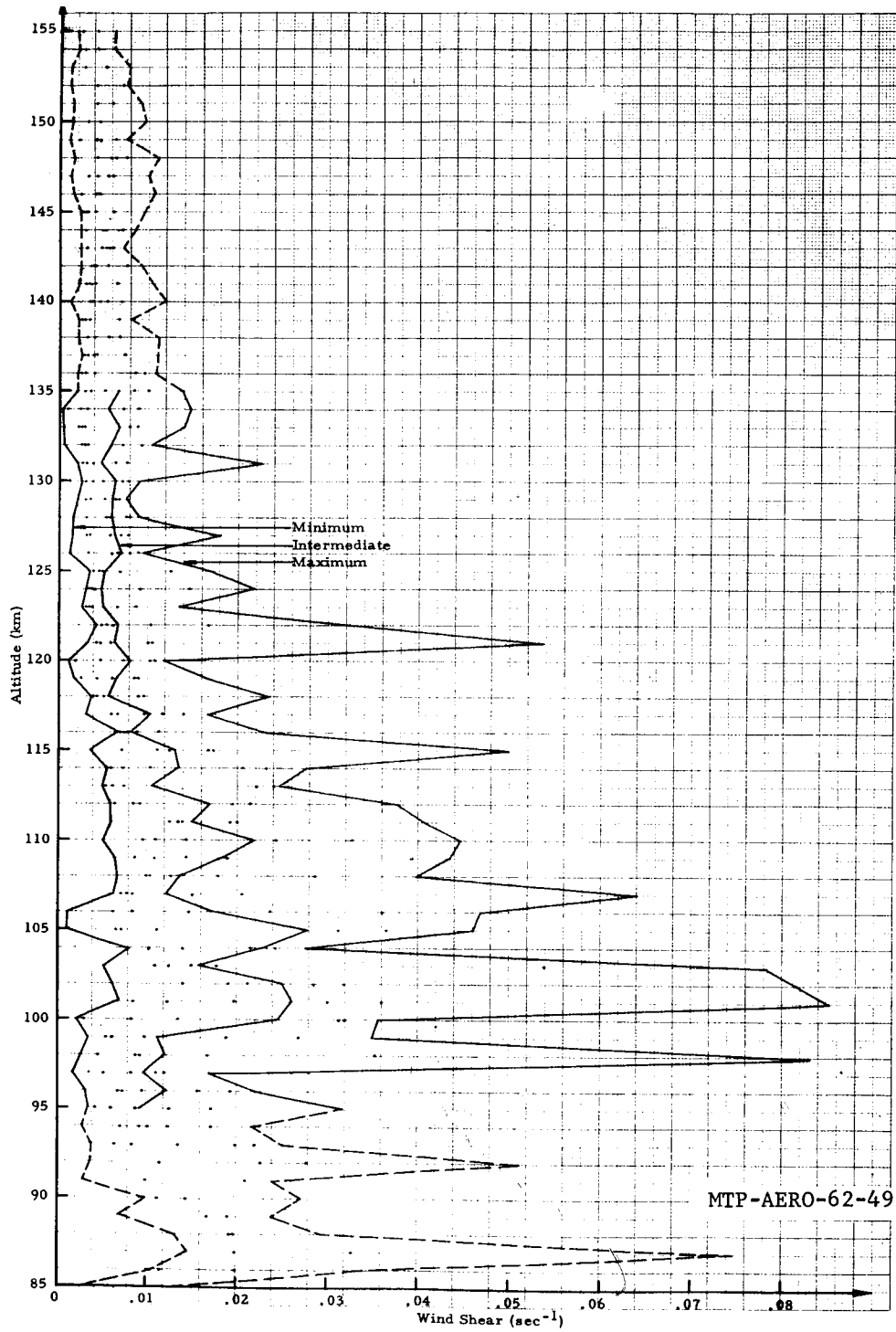


FIG. 16. WIND SHEAR ENVELOPES OBTAINED FROM SODIUM VAPOR TRAIL MEASUREMENTS AT WALLOPS ISLAND, VIRGINIA FOR 1000 m ALTITUDE LAYERS ( $\Delta h$ )

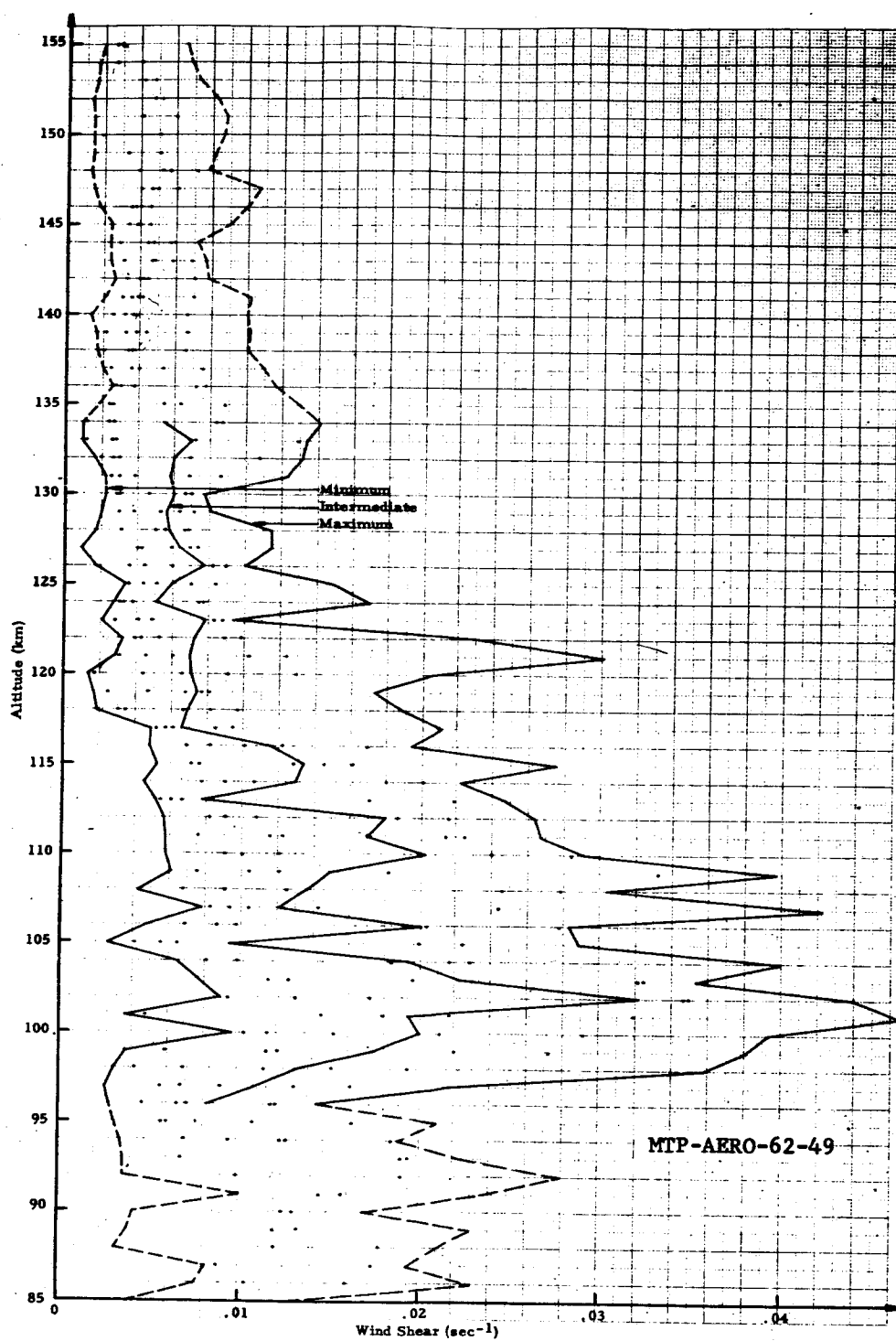


FIG. 17. WIND SHEAR ENVELOPES OBTAINED FROM SODIUM VAPOR TRAIL MEASUREMENTS AT WALLOPS ISLAND, VIRGINIA FOR 3000 m ALTITUDE LAYERS ( $\Delta h$ )

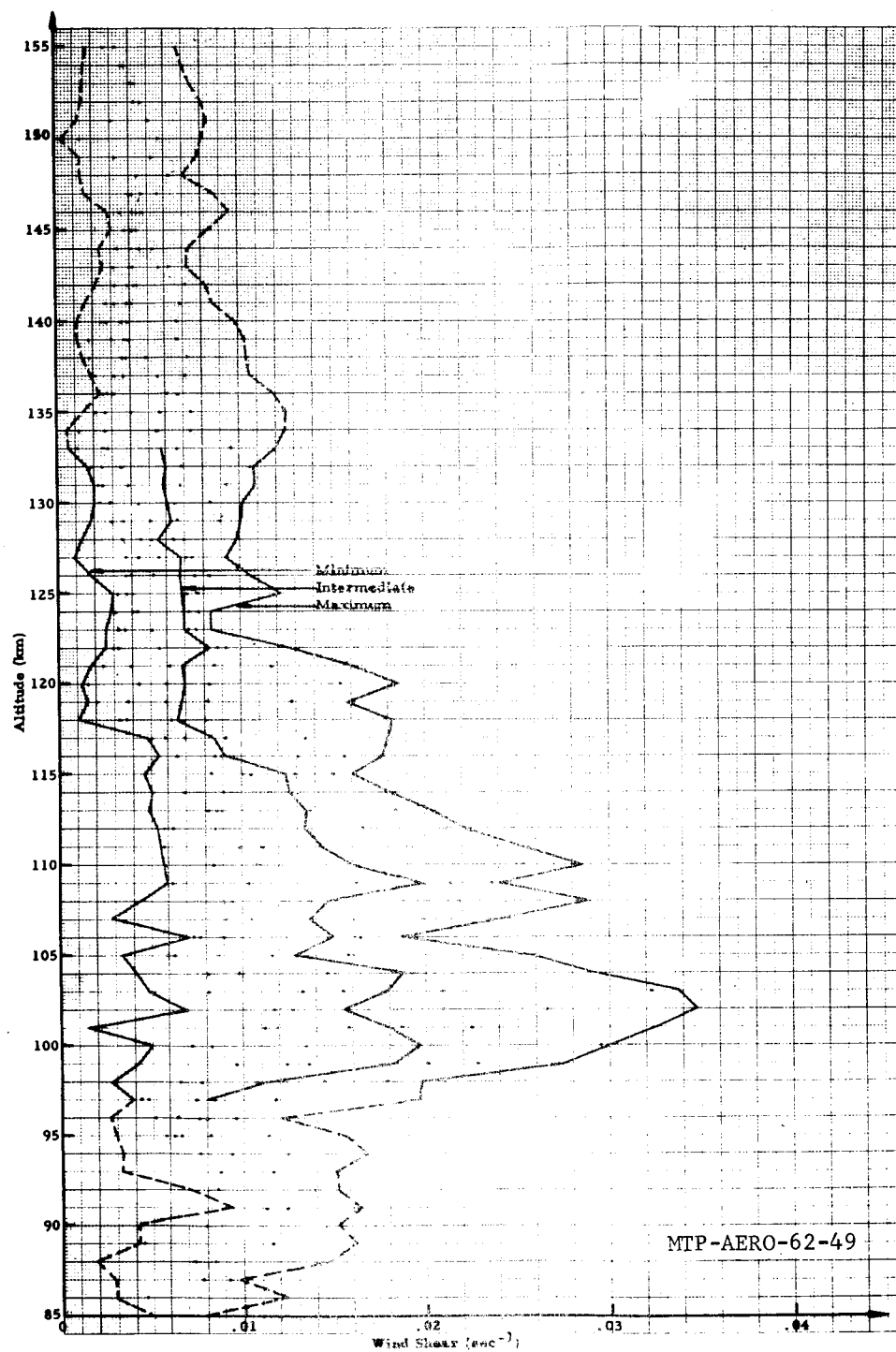


FIG. 18. WIND SHEAR ENVELOPES OBTAINED FROM SODIUM VAPOR TRAIL MEASUREMENTS AT WALLOPS ISLAND, VIRGINIA FOR 5000 m ALTITUDE LAYERS ( $\Delta h$ )

## REFERENCES

1. Scoggins, J. R., and W. W. Vaughan, "Cape Canaveral Wind and Shear Data (1 thru 80 km) for Use in Vehicle Design and Performance Studies, "NASA TN D-1274.
2. Johnson, F. S., Satellite Environment Handbook, Stanford University Press, Stanford, California, 1961.
3. Kallman, H. K., "Recent Results of High Altitude Research by Means of Rockets and Satellites," RM-2275, ASTIA
4. Maxwell, A., and M. Dagg, "A Radio Astronomical Investigation of Drift Movements in the Upper Atmosphere," Phil Mag, Vol. 45, No. 365, pp. 551-569, June 1954.
5. Kushnerevskiy, Yu. V., and Ye. S. Zayarnaya, "Drift of Small-Scale Irregularities in the F-2 Layer," NASA-TT F-20, pp. 27-44, June 1960.
6. Thomas, L., "Some Measurements of Horizontal Movements in Region F-2 Using Widely Spaced Observing Stations," J. Atmos. & Ter. Phys., Vol. 14, pp. 123-137, 1961.
7. Becken, J., and B. Maehlum, "Drift Measurements at Kjeller on the Ionospheric F-Region," J. Geophys. Res. Vol. 65, No. 5, pp. 1485-1488, May 1960.
8. Purslow, B. W., "Ionospheric Drift in the F-2 Region Near the Magnetic Equator," Nature, No. 4601, pp. 35-36, January 4, 1958.
9. Beynon, W. J. G., "Evidence of Horizontal Motion in Region F-2 Ionization," Nature, No. 4127, Vol. 162, p. 887, December 4, 1948.

10. Rao, B. Ramachandra, and E. Bhagiratha Rao, "Study of Horizontal Drifts in the ( $F_1$  and  $F_2$ ) Regions of the Ionosphere at Waltair ( $17^\circ 43'$  N,  $83^\circ 18'$  E, Mag. Lat.  $9^\circ 30'$  N)," J. Atmos. & Ter. Phys., Vol. 14, pp. 94-106, 1959.
11. Kashcheyev, B. L., N. T. Tsymbal, and Ye. G. Proshkin, "Study of the Ionosphere Above Khar'kov During the IGY Period," NASA Technical Translation F-20, pp. 54-69, June, 1960.
12. Singh, R. N. , and S. R. Khastgir, "Study of Winds in the F-Region of the Ionosphere During the Unusual Days in the IGY-Calendar," J. Atmos. & Ter. Phys., Vol. 18, pp. 29-42, 1960.
13. Osborne, B. W., "Horizontal Movements of Ionization in the Equatorial F-Region," J. Atmos. & Ter. Phys., Vol. 6, pp. 117-123, 1955.
14. Harvey, J. A., "Movement of Sporadic E. Ionization," Aust. J. Phys., Vol. 8, No. 4, pp. 523-534, July 18, 1955.
15. Munro, G. H., "Traveling Disturbances in the Ionosphere," Proc. Phys. Soc., London, Vol. A 202, pp. 208-223, 1950.
16. Yerofeyev, N. M., G. G. Dzhemilev, V. P. Perelygin, and V. P. Petinov, "Original Results of Radiotechnical Observations of the Movement of Irregularities in the Ionosphere (Winds) Over Ashkhabad at Altitudes of 200-300 km," NASA Technical Translation F-20, pp. 45-53, June, 1960.
17. Toman, Kurt, "Movement of the F-Region," J. Geophys. Res., Vol. 60, No. 1, pp. 57-70, March, 1955.
18. Shearman, E. D. R., and J. Harwood, "Sporadic-E as Observed by Back-Scatter Techniques in United Kingdom," J. Atmos. & Ter. Phys., Vol. 18, pp. 29-42, 1960.
19. Phillips, G. J., "Measurements of Winds in the Ionosphere," J. Atmos. & Ter. Phys., Vol. 2, pp. 141-154, 1952.



20. Obayashi, T., "Movements of Irregularities in the E Region," *Journal of the Radio Research Laboratories*, Vol. 2, No. 7, pp. 59-67, January, 1955.
21. Yerg, Donald G., "Notes on Correlation Methods for Evaluating Ionospheric Winds from Radio Fading Records," *J. Geophys. Res.*, Vol. 60, No. 2, pp. 173-185, June 1955.
22. Thomas, J. A. and M. J. Burke, "Motion in the Night-time E<sub>s</sub> Region at Brisbane," *Aust. J. Phys.*, Vol. 9, pp. 440-453, August 6, 1956.
23. Checha, V. A. and V. Ye. Zelenkov, "Drifts of Irregularities in the Ionosphere According to Observations of the Tomsk Ionospheric Station," *NASA Technical Translation F-20*, pp. 70-83, June, 1960.
24. Harwood, J., "Some Observations of the Occurrence and Movement of Sporadic E Ionization," *J. Atmos. & Ter. Phys.*, Vol. 20, pp. 243-262, 1961.
25. Mitra, S. N., "A Radio Method of Measuring Winds in the Ionosphere," *Proc. Inst. Elect. Engrs.*, Vol. 96, Part III, pp. 441-446, February, 1949.
26. Manning, L. A., O. G. Villard, Jr., A. M. Peterson, "Meteoric Echo Study of Upper Atmosphere Winds," *Proc. of the I. R. E.*, Vol. 38 (8), pp. 877-883, August, 1950.
27. Greenhow, J. S. and E. L. Neufeld, "Measurements of Turbulence in the 80-100 km Region from the Radio Echo Observations of Meteors," *J. Geophys. Res.*, Vol. 64, No. 12, pp. 2129-2133, December, 1959.
28. Elford, W. G., "A Study of Winds Between 80 and 100 km in Medium Latitudes," *Planetary and Space Sciences*, Vol. 1, pp. 94-101, 1959.
29. Hudson, G. E., S. Weisbrod, J. L. Heritage, and J. Zane, "A Study of High Altitude Wind Research-Part I-Methods and Bibliography," *Final Technical Report No. SRA-30*, Smyth Research Associates, California, June 12, 1956-January 12, 1957.

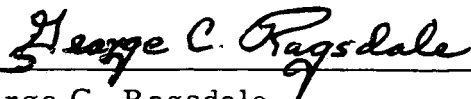
30. Nordberg, W. and W. G. Stroud, "Results of IGY Rocket-Grenade Experiments to Measure Temperatures and Winds Above the Island of Guam," J. Geophys. Res., Vol. 66, No. 2, pp. 455-464, February, 1961.
31. Stroud, W. G., W. Nordberg, W. R. Bandeen, F. L. Bartman, and P. Titus, "Rocket-Grenade Measurements of Temperatures and Winds in the Mesosphere over Churchill, Canada," J. Geophys. Res., Vol. 65, No. 8, pp. 2307-2323, August, 1960.
32. Manring, E., J. Bedinger, H. Knafllich, and R. Lynch, "Upper Atmospheric Wind Profiles Determined from Three Rocket Experiments," GCA Technical Report, February, 1961.
33. Nordberg, W., "Results of Meteorological Rocket Measurements above 60 km," A Paper Presented at the International Symposium on Rocket and Satellite Meteorology, Washington, D. C., April 23-25, 1962.
34. Graphs of wind speeds and direction observed at Wallops Island, Virginia, were furnished by W. Nordberg, W. Smith, and E. Manring as the result of private communications on October 26, 1961, and January 24, 1962.
35. Champion, K. S. W., and S. P. Zimmerman, "Winds and Turbulence at 200,000 to 400,000 Feet from Chemical Releases," Paper Presented at the Symposium on "Winds for Aerospace Vehicle Design," at L. G. Hanscom Field, Bedford, Massachusetts, on September 27-28, 1961.
36. Moore, C. B., "Some Wind Determinations in the Upper Atmosphere Using Artificially Generated Sodium Clouds," J. Geophys. Res., Vol. 64, pp. 584-591, June, 1959.
37. Whipple, F. L., "Evidence for Winds in the Outer Atmosphere," Procedure of the National Academy of Science, Vol. 40, pp. 966-972, 1954.
38. Liller, William, and Fred L. Whipple, "High Altitude Winds by Meteor-Train Photography," Special Supplement to J. Geophys. Res., Vol. 64, No. 12, pp. 2122-2128, December, 1959.

39. Mitra, S. K., "The Upper Atmosphere," The Asiatic Society, Calcutta, India, Second Edition, 1952.
40. Sharonov, V. V., "The Dependence of the Frequency of Appearance of Noctilucent Clouds Upon the Date and the Geographical Latitude," NASA Technical Translation F-50, pp. 1-6, November, 1960.
41. Stormer, Carl, "Measurements of Luminous Night Clouds in Norway '33 & '34," *Astrophysica Norvegica*, Vol. I, No.3 pp. 88-115, 1935.
42. Smith, L. B., "Monthly Observations of Winds Between 100,000 and 300,000 Feet," Research Report SC-4482(RR), Sandia Corp., September, 1960.
43. Greenhow, J. S., "Systematic Wind Measurements at Altitudes of 80-100 km Using Radio Echoes from Meteor Trails," *Phil. Mag.*, Vol. 45, No. 364, pp. 471-490, May, 1954.
44. Greenhow, J. S. and E. L. Neufeld, "Turbulence in the Lower E-Region from Meteor Echo Observations," Electromagnetic Wave Propagation, Academic Press, pp. 493-504, 1960.
45. Greenhow, J. S. and E. L. Neufeld, "The Height Variation of Upper Atmospheric Winds," *Phil. Mag.*, Vol. 1, pp. 1157-1171, 1956.
46. Elford, W. G. and D. S. Robertson, "Measurements of Winds in the Upper Atmosphere by Means of Drifting Meteor Trails II," *J. Atmos. & Terr. Phys.*, Vol. 4, pp. 271-284, 1953.
47. Seddon, J. Carl, "Summary of Rocket and Satellite Observations Related to the Ionosphere," NASA Technical Note D-667, January, 1961.
48. Dueno, Braulio, "Measurement of Ionospheric Drift by Radio-Star Observations," *J. Geophys. Res.*, Vol. 66, No. 8, pp. 2355-2365, August, 1961.

49. Batten, E. S., "Wind Systems in the Mesosphere and Lower Ionosphere," *Journal of Meteorology*, Vol. 18, pp. 283-291, June, 1961.
50. Vaughan, William W., "Wind Profiles at Staging Altitudes (35 km to 80 km)," NASA Publication prepared for presentation to National Symposium on "Winds for Aerospace Vehicle Design," at L. G. Hanscom Field, Bedford, Massachusetts, on September 27-28, 1961.
51. Broglio, L., "Review of Italian Meteorological Activities and Results," Commissione per le Ricerche Spaziali Scuola d'Ingegneria Aeronautica, Rome, Italy. A paper presented at the International Symposium on Rocket and Satellite Meteorology, Washington, D. C., April 23-25, 1962.
52. Millman, P. M., "Visual and Photographic Observations of Meteors and Noctilucent Clouds," *J. Geophys. Res.*, Vol. 64, No. 12, pp. 2122-2128, December, 1959.
53. Ratcliffe, J. A., "Ionizations and Drifts in the Ionosphere," *J. Geophys. Res.*, Vol. 64, No. 12, pp. 2102-2111, December, 1959.
54. Briggs, B. H. and M. Spencer, "Horizontal Movements in the Ionosphere," *Reports on Progress in Physics*, Vol. 17, pp. 245-280, 1954.
55. Chapman, J. H., "A Study of Winds in the Ionosphere by Radio Methods," *Canadian Journal of Physics*, Vol. 31, pp. 120-131, 1953.

## APPROVAL

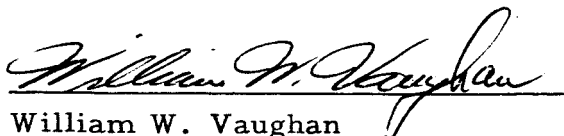
The information in this report has been reviewed for security classification. Review of any information concerning Department of Defense or Atomic Energy Commission programs has been made by the MSFC Security Classification Officer. This report, in its entirety, has been determined to be unclassified.



George C. Ragsdale



Peter E. Wasko  
Chief, Space Environment Section



William W. Vaughan  
Chief, Aerophysics & Astrophysics Branch



E. D. Geissler  
Director, Aeroballistics Division

## DISTRIBUTION

## INTERNAL

M-DEP-R&amp;D

M-TPC

M-SAT (6)

M-FPO (3)

M-COMP (3)

M-L&amp;M (3)

M-RP (6)

M-CP (3)

M-AERO

Dr. Geissler

Dr. Hoelker (2)

Mr. Jean (2)

Mr. Miner

Mr. Winch

Mr. Teague

Mr. Callaway

Mr. Schmieder

Mr. Horn (2)

Mr. Bauer

Mr. Golmon

Mr. Baker

Mr. Hart

Mr. Stone

Mr. Dahm (2)

Mr. Linsley

Mr. Wilson

Dr. Adams

Dr. Speer (2)

Mr. Lindberg

Mr. Fulmer

Mr. Kurtz (2)

Mr. Holderer (2)

Mr. Vaughan (10)

Mr. Scoggins

Mr. Baussus

Mr. Schow

Mr. R. Turner

Mr. C. Dalton

Mr. Larsen

Dr. Heybey

Mr. Cummings

Mr. O. Smith

Mr. P. Wasko (30)

Mr. Braunlich (2)

Mr. J. Smith

Mr. Douglas

Mr. C. Collins

Mr. G. Ragsdale (15)

Mr. T. Reed

Mr. W. Murphree

M-ASTR

Dr. Haeussermann (2)

Mr. Hosenthien (3)

Mr. Digesu

Mr. Mandel

Mr. W. Wagon

Mr. H. Hood

Mr. Hoberg (2)

Mr. Moore (2)

M-P&amp;VED

Col. Fellows (2)

Mr. Mrazek (2)

Mr. Weidner

Mr. Hellebrand

Mr. R. Gause

Mr. E. McKannan

Mr. Goerner (2)

Mr. Kroll (2)

Mr. Palaoro (2)

Mr. Pedigo

Mr. Hannaford

Mr. R. Hunt

M-TEST

Mr. Heimburg

Dr. Sieber

Mr. F. Kramer

Mr. J. Conner

## M-LOD

Dr. Debus (2)

Dr. Bruns

Dr. Gruene

Dr. Knothe (2)

Mr. Sendler

Col. Gibbs

Mr. Poppel

Mr. Claybourne

Mr. Abercrombie

Mr. Taiani

Maj. Petrone (2)

Mr. Hershey

Mr. Zeiler

Mr. Gorman

M-MS-IPL (8)

M-MS-IP

M-MS-H

M-PAT

M-HME-P

## DISTRIBUTION

## EXTERNAL

NASA Headquarters  
Federal Office Building Number 6  
Washington 25, D. C.  
Attn: Technical Information Division (2)

NASA  
Office of Manned Space Flight  
Federal Office Building Number 6  
Washington 25, D. C.  
Attn: Director  
    Mr. Joseph Shea  
    Mr. Milton Rosen  
    Mr. George Low  
    Mr. Roadman

NASA  
Office of Applications  
Federal Office Building Number 6  
Washington 25, D. C.  
Attn: Director  
    Dr. Morris Tepper (2)  
    Mr. Wm. Spreen

NASA  
Office of Space Sciences  
Federal Office Building Number 6  
Washington 25, D. C.  
Attn: Dr. Homer E. Newell  
    Mr. John Clark  
    Mr. Donald Heaton  
    Mr. Maurice Dubin

NASA  
Manned Spacecraft Center  
Houston 1, Texas  
Attn: Director (2)  
    Mr. R. Thompson (2)  
    Mr. D. Cheatham  
    Mr. Benjamin Chereek  
    Mr. Francis Casey  
    Mr. Paige Burbank



## EXTERNAL

NASA

Langley Research Center  
Langley Field, Virginia

Attn: Director (2)

Mr. Harry Runyan  
Mr. H. B. Tolefson  
Mr. T. Coleman  
Mr. Richard Hord  
Dr. John E. Duberg

National Weather Records Center

Arcade Building  
Asheville, North CarolinaAttn: Dr. Barger  
Dr. Crutcher

NASA

Ames Research Center  
Moffett Field, California

Attn: Director (2)

Mr. Manley Hood

NASA

Jet Propulsion Laboratory  
4800 Oak Grove Dr.  
Pasadena, California

Attn: Director (2)

Mr. Herbert Trostle  
Mr. Conway Snyder

U. S. Weather Bureau

Office of Climatology  
Washington 25, D. C.

Attn: Dr. Landsberg

Pan American World Airways

Division Meteorologist  
Patrick Air Force Base, FloridaAttn: Mr. Gerald Finger  
Mr. O. H. Daniels

NASA

Lewis Research Center  
Cleveland, Ohio

Attn: Director

Dr. Rinaldo Brun

## EXTERNAL

Dr. Hans A. Panofsky  
1179 Oneida Street  
State College, Pennsylvania

North American Aviation, Inc.  
Thru: MSFC Saturn Projects Office

Douglas Aircraft Corporation  
Thru: MSFC Saturn Projects Office

Mr. Ernest Ammon  
U. S. Weather Bureau  
NASA Manned Spacecraft Center  
Cape Canaveral, Florida

Office of Advanced Research and Technology  
1520 H Street, N. W.  
Washington 25, D. C.  
Attn: Director (2)  
Mr. Charak  
Mr. H. B. Finger  
Mr. Milton Ames  
Mr. Richard Rhode (2)

NASA  
Goddard Space Flight Center  
Greenbelt, Maryland  
Attn: Director  
Dr. W. Nordberg (2)  
Dr. Spencer  
Mr. John C. New  
Mr. J. Gosset (5)  
Mr. W. S. Smith  
Library

AOMC Research Library (2)  
ORDXM-RB  
Building 4488

## EXTERNAL

Air Force Cambridge Research Labs  
L. G. Hanscom Field  
Bedford, Massachusetts  
Attn: Mr. Norman Sissenwine  
Dr. Arnold Court  
Mr. Robert Leviton  
Dr. Martin Barad  
Dr. Champion (2)  
Mr. T. J. Keegan

Air Force Missile Test Center  
Patrick AFB, Florida  
Attn: L/Col Peter Romo  
Det. 11, 4th Weather Group  
Captain Christensen

Major William Gommel  
Headquarters, DCAS (DCLW)  
Air Force Unit Post Office  
Los Angeles 45, California

Aeronautical Systems Division  
Wright Patterson AFB, Ohio  
Attn: Director  
Mr. H. G. Kasten

Dr. David Woodbridge  
Staff Scientist for Space Environment  
Chance Vought Corp.  
P. O. Box 5907  
Dallas 22, Texas

Mr. Sol Lutwak  
Space Technology Laboratories, Inc.  
Building R-1, Room 1028  
One Space Park  
Redondo Beach, California

## EXTERNAL

Boeing Aircraft Company  
Thru: MSFC Saturn Project Office

Lockheed Aircraft Corporation  
Thru: L & M Office

Climatic Center, USAF  
Air Weather Service (MATS)  
Annex 2, 225 D Street, S. E.  
Washington 25, D. C.  
Attn: CCDID

Lt. Col. Robert Durbin (2)  
Headquarters  
Air Weather Service  
Scott Air Force Base, Illinois

Director (2)  
Meteorological Division  
U. S. Army Signal R & D Laboratory  
Fort Monmouth New Jersey

Dr. O. Essenwanger (2)  
AOMC Research Laboratory  
Redstone Arsenal, Alabama

AOMC Research Library (2)  
ORDXM-RB  
Building 7120

Convair General Dynamics  
Thru: L & M Office

Mr. E. S. Batten  
Rand Corporation  
Santa Monica, California

Mr. Lawrence B. Smith (2)  
Sandia Corporation  
Albuquerque, New Mexico